Published in final edited form as:
Dev Dyn. 2013 February ; 242(2): 132–147. doi:10.1002/dvdy.23910.

Correct Timing of Proliferation and Differentiation is Necessary for Normal Inner Ear Development and Auditory Hair Cell Viability

Benjamin J. Kopecky[1,2,*], **Israt Jahan**[1], and **Bernd Fritzsch**[1]

[1]University of Iowa, Department of Biology, Iowa City, IA, USA

[2]University of Iowa Carver College of Medicine, Medical Scientist Training Program, Iowa City, IA, USA

Abstract

Background—Hearing restoration through hair cell regeneration will require revealing the dynamic interactions between proliferation and differentiation during development to avoid the limited viability of regenerated hair cells. *Pax2-Cre N-Myc* conditional knockout (CKO) mice highlighted the need of *N-Myc* for proper neurosensory development and possible redundancy with *L-Myc*. The late-onset hair cell death in the absence of early *N-Myc* expression could be due to mis-regulation of genes necessary for neurosensory formation and maintenance, such as *Neurod1, Atoh1, Pou4f3,* and *Barhl1*.

Results—*Pax2-Cre N-Myc L-Myc* double CKO mice show that proliferation and differentiation are linked together through *Myc* and in the absence of both *Mycs*, altered proliferation and differentiation results in morphologically abnormal ears. In particular, the organ of Corti apex is re-patterned into a vestibular-like organization and the base is truncated and fused with the saccule.

Conclusions—These data indicate that therapeutic approaches to restore hair cells must take into account a dynamic interaction of proliferation and differentiation regulation of basic Helix-Loop-Helix transcription factors in attempts to stably replace lost cochlear hair cells. In addition, our data indicate that *Myc* is an integral component of the evolutionary transformation process that resulted in the organ of Corti development.

Keywords

L-Myc; N-Myc; Hair Cell; Hearing; Prevention; Regeneration

Introduction

Hearing loss is a major epidemiologic problem worldwide that greatly affects hundreds of millions of peoples' quality of life. Two major forms of hearing loss exist: conductive and sensorineural. While both pose problems to individuals, sensorineural hearing loss (SNHL) is irreversible due to the damage of sensory hair cells in the inner ear. SNHL varies from mild to profound thus allowing for the success of modern day cochlear implants which function through remaining auditory neurons. Despite massive improvements, cochlear implants are still unable to fully recapitulate normal hearing (Roehm and Hansen, 2005;

*Corresponding Author: Benjamin Kopecky, Department of Biology, College of Liberal Arts and Sciences, 331 BB, Iowa City, IA, 52242, USA, benjamin-kopecky@uiowa.edu.

Chang and Fu, 2006; Bent et al., 2009; Gifford and Revit, 2010; Peterson et al., 2010; Renton et al., 2010; Colletti et al., 2011). Thus, while cochlear implants improve patients' auditory function and quality of life, the only permanent and perfect hearing restoration treatment is the regeneration of the damaged or lost organ of Corti to reform the 'world's best hearing aid' (Puligilla and Kelley, 2009).

The organ of Corti is composed of hair cells, supporting cells, and neurons, all of which need to be properly formed and maintained for hearing to occur. In patients with short-term hearing loss, it is possible that only hair cells would need to be replaced; however, in patients with long-term hearing loss, the entire organ of Corti may be lost (Izumikawa et al., 2008). Regardless, therapy may require the ability to recapitulate critical developmental steps of the organ of Corti *in vivo* to manipulate a naïve stem cell, stem cell like-cell or an induced post-mitotic inner ear cell towards each individual cell fate (Kopecky et al., 2011). To accomplish this, it may be necessary to elucidate more critically the embryonic developmental molecular network that initially formed the organ of Corti. Many of the early developmental steps that define the otic placode, inner ear axis specification, organ of Corti patterning, and even the neurosensory precursor populations, remain ill-defined.

The initial precursor population size of the organ of Corti is unknown; however, the end-product of development is roughly 15,000 hair cells in humans, divided into three rows of outer hair cells and one row of inner hair cells surrounded by several types of supporting cells. This organization is uniform along the several millimeters of the organ of Corti that stretches for over two complete turns from base to apex forming a sound frequency distribution map along its length. The stereotyped pattern of the organ of Corti across all mammals indicates that development is under tight genetic control and is not a stochastic process. To date, numerous studies have revealed that this developmental process requires diffusible factors that define the boundaries of the organ of Corti (Morsli et al., 1998; Pirvola et al., 2000; Pauley et al., 2003; Pan et al., 2011; Groves and Fekete, 2012) and a set of transcription factors that first, determine the proliferation of the precursor populations, second, differentiate subpopulations of the precursor pool into hair cells, third, form cell-cell interactions to stabilize the cell fate of hair cells and supporting cells, and last, provide long-term support to maintain the viability of this fragile and complex organ of Corti (Fritzsch et al., 2011). Each of these steps are interconnected to the steps before it as mouse models with mutations in upstream genes produce cumulative effects of downstream abnormalities. Therefore, perhaps the most important step for not only the proper development of the inner ear, but also for hair cell regeneration, is the highly complex modulation of proliferation, arguably the least understood part of ear development. Our current study focuses on the molecular interaction between the proliferation of neurosensory precursor populations, differentiation of these neurosensory precursors into hair cells, and how this delicate interaction may affect long-term maintenance of the organ of Corti.

Proliferation is the act of guiding a cell through the highly redundant and tightly regulated cell cycle. It is regulated through multiple cell cycle checkpoints and through both genetic and epigenetic mechanisms. Manipulation of proliferation throughout the ear in many species has been attempted through either exogenous mitogens such as the EGFs and FGFs (Zheng et al., 1997; Montcouquiol and Corwin, 2001; Witte et al., 2001) or through direct cell cycle regulation (Chen et al., 2003; Mantela et al., 2005; Sage et al., 2006; Oesterle et al., 2011). Various studies have been able to force continued proliferation of embryonic precursor cells or restart later proliferation of either supporting cells or in rare cases, hair cells (Liu et al., 2012). Neither method was able to consistently provide long-term success as a common outcome of hair cells formed after manipulation of proliferation, was cell death (Chen et al., 2003; Mantela et al., 2005; Sage et al., 2006; Weber et al., 2008; Oesterle et al., 2011). Other manipulations simply proved ineffective after a certain stage in development

(White et al., 2006). Perhaps a node integrating many of these upstream signals (*i.e.* EGFs and FGFs) that synergize into important cell cycle control (*i.e.* Cyclins, pRB, and E2Fs) may mitigate these side effects and could achieve late induction of proliferation of organ of Corti cells. Indeed, the *Myc* node is upstream of many cell cycle regulating genes and possibly could provide insight into the underexplored balance between proliferation and differentiation during development (Conacci-Sorrell and Eisenman, 2011; Young et al., 2011). Unlike any other proto-oncogene or cell cycle regulatory gene previously analyzed (Pauley et al., 2006; Laine et al., 2007; Rocha-Sanchez et al., 2011), the *Myc's* are bHLH transcription factors that bind specifically to E-boxes that are part of the promoters of target genes. Three bHLH transcription factors, *Neurogenin1, Neurod1*, and *Atoh1*, are essential for the differentiation of neurons and hair cells in the ear (Fritzsch et al., 2010) and these class II bHLH genes bind to a nearly identical class of E-boxes as the *Mycs*. Furthermore, immediately downstream to *Myc* are Inhibitors of Differentiation and DNA binding (*Ids*), which are known to directly inhibit class II bHLH transcription factors (Fritzsch et al., 2006; Jones et al., 2006) through interactions with the E-proteins needed for E-box binding of class II bHLH factors (Bhattacharya and Baker, 2011). Additionally, two genes, *Eya1* and *Six1,* are sufficient for neuronal and hair cell formation in addition to bHLH expression (Ahmed et al., 2012a; Ahmed et al., 2012b) and may also regulate *Myc* expression. Thus, the *Mycs* appear to be a key node that balances proliferation and differentiation and therefore, manipulations of the *Mycs* may not only affect the level of proliferation in the ear, but also the onset of differentiation. Until recently, *Myc* function in the ear had been unstudied.

We have previously explored the effect of *N-Myc* in the inner ear using *Pax2-Cre* to conditionally delete *N-Myc* (Kopecky et al., 2011). A parallel study (Dominguez-Frutos et al., 2011) confirmed that *N-Myc* mutants had a severe reduction in size, abnormal morphogenesis, including a truncated cochlea with multiple rows of hair cells, a fused utricle, saccule, and base of the cochlea, and the loss of the horizontal canal (Kopecky et al., 2011). *N-Myc* and *L-Myc* are mostly co-expressed and are detected as early as embryonic day (E) 8.5 (Dominguez-Frutos et al., 2011). *N-Myc* and *L-Myc* are subsequently restricted to prosensory and then exclusively expressed in the sensory epithelia (Dominguez-Frutos et al., 2011; Kopecky et al., 2011). Despite the aberrant morphology, the *Pax2-Cre N-Myc* conditional knockout (CKO) mice developed both cochlear as well as vestibular hair cells; however, cochlear hair cells were progressively lost starting around postnatal day (P) 14, whereas vestibular hair cells were retained until at least nine months of age (Kopecky et al., 2011). These mice were deaf and suffered from partially compensated ataxic gait (Kopecky et al., 2012a). From these initial studies, it was apparent that *N-Myc* and *L-Myc* but not *C-Myc* were expressed strongly in the inner ear and that this co-expression may have a potential redundant function during development. Furthermore, expression of both *N-Myc* and *L-Myc* in hair cells after birth coupled with the late loss of cochlear hair cells suggested a potential late-onset effect of *N-Myc* and *L-Myc* in long-term hair cell maintenance; an observation that could have significant translational impacts(Kopecky et al., 2011). We therefore generated two additional mouse models, one of which knocked out *N-Myc* and *L-Myc* in hair cells after hair cell differentiation using the previously described *Atoh1-Cre* (Matei et al., 2005) and the other one is using *Pax2-Cre*. *Atoh1-Cre* upregulation is much later than *Pax2-Cre* and *Atoh1* is specifically expressed in inner ear hair cells whereas the *Pax2* is expressed in the pro-sensory region in the otic placode as early as E8.5. Delayed deletion of *N-Myc* and *L-Myc* in hair cells using *Atoh1-Cre* would test whether the hair cell loss seen in the *Pax2-Cre N-Myc* CKO mice was due to a late-onset effect of the *Mycs* specifically in hair cells. However, the late expression of *N-Myc* and *L-Myc* in hair cells likely does not play a direct role in long-term hair cell viability as there is no loss of cochlear hair cells in delayed deletion (Kopecky et al., 2012c). There is also no additional loss of cochlear hair cells in *Atoh1-Cre N-Myc f/f L-Myc f/f* mouse even with the

administration of ototoxic drug (Kopecky et al., 2012c). This suggested that the survival of cochlear hair cells is possibly due to the balance between proliferation and differentiation that is set up by very early expression of *N-Myc* and *L-Myc* during development. We test this hypothesis by knocking out *N-Myc* and/or *L-Myc* with *Pax2-Cre* and subsequently assessing important markers of both proliferation and differentiation throughout the time course of hair cell formation.

In the present study, we consider the relative compensatory abilities of *N-Myc* and *L-Myc* during development in conditional knock outs of *N-Myc* and/or *L-Myc* using *Pax2-Cre*, the overall loss of proliferation in the *Pax2-Cre N-Myc f/f L-Myc f/f* double (d) CKO mice, and how the loss of both *N-Myc* and *L-Myc* affect the balance between proliferation and differentiation. Our data indicate that the function of *L-Myc* can be compensated by that of *N-Myc* but *L-Myc* cannot compensate the function of *N-Myc*. However, the *Pax2-Cre N-Myc f/f L-Myc f/f* dCKO mice have a more severe cochlear phenotype than in the previously described *Pax2-Cre N-Myc* single CKO mice and are never viable thus limiting postnatal investigations of long-term hair cell viability.

Results

In this paper we compared the roles of *N-Myc* and *L-Myc* using different combinations of mutant alleles by the *Pax2-Cre* mediated recombination such as *Pax2-Cre N-Myc f/+ L-Myc f/f, Pax2-Cre L-Myc f/f, Pax2-Cre N-Myc f/f L-Myc f/+, and Pax2-Cre N-Myc f/f L-Myc f/f* mice. However, neither *N-Myc* nor *L-Myc* single or double heterozygous mice has any phenotype neither do they have any added effect if *N-Myc* heterozygous mice combined with *L*-Myc's homozygosity as compared between *Pax2-Cre N-Myc f/+ L-Myc f/f* and *Pax2-Cre L-Myc f/f*. We therefore termed *Pax2-Cre N-Myc f/+ L-Myc f/f* or *Pax2-Cre L-Myc f/f* mice as '*L-Myc* CKO', *Pax2-Cre N-Myc f/f L-Myc f/+* mice as '*N-Myc* CKO' and *Pax2-Cre N-Myc f/f L-Myc f/f* mice as 'dCKO' for the simplicity of the genotype in the rest of the paper. *Pax2-Cre N-Myc f/f* mice as described in Kopecky et al, 2011 and Dominguez-Frutos et al, 2011 will be still written out to avoid confusion. *N-Myc f/+ L-Myc f/+* mice without *Cre* are used as 'control'.

Combined Loss of *N-Myc* and *L-Myc* Results in a More Disrupted Inner Ear than Loss of Either *N-Myc* or *L-Myc* Alone

We generated three dimensional reconstructions using confocal microscopy allowing for non-destructive optical sectioning of high resolution images and easy three dimensional manipulations and quantification of control, *L-Myc* CKO, *N-Myc* CKO, and dCKO ears from E11.5 to E18.5 to assess the development of the inner ear in the absence of either *N-Myc* or *L-Myc* or both. From E11.5 to E18.5, control development was identical to that previously described using the scanning Thin-Sheet Laser Imaging Microscopy (sTSLIM) technique (Kopecky et al., 2012b). At E11.5, the control inner ear was an otocyst with all axes defined. By E12.5, the ventral elongation of the cochlea became apparent. At this age, the dorsal vestibular canals began forming and the endolymphatic duct was prevalent. From E13.5 to E16.5, the inner ear grew and obtained a more mature form such that by E16.5, all sensory recesses were able to be uniquely identified with the formation of the ductus reuniens and utriculosaccular foramen (Fig. 1, row 1). In the *L-Myc* CKO developmental series, we knocked out *L-Myc*; however, no noticeable morphologic changes were apparent compared to age matched controls (Fig. 1, row 2). However, when we assessed the *N-Myc* CKO developmental series, where the inner ear developed in the absence of *N-Myc*, there were dramatic developmental abnormalities as early as E11.5 (Fig. 1, row 3). The inner ear was drastically reduced in size and both the ventral and dorsal compartments were disrupted. No prominent saccular recess formed and the cochlear elongation was stunted, with a prominent circularization at the apex, sometimes completely disconnected from the middle

turn, as seen in E18.5. Neither the ductus reuniens nor the utriculosaccular foramen formed, and thus, there was no morphologically distinct utricle, saccule, and base of the cochlea, but rather a continuum of these epithelia. Despite the lack of effect when *L-Myc* was knocked out alone in the *L-Myc* CKO mice, when *L-Myc* was knocked out in conjunction with *N-Myc* in the dCKO mice, the loss of *L-Myc* appeared to have an additive effect (Fig. 1, row 4). When both *Mycs* were knocked out, there were increased developmental disruptions in the vestibular canals. In the *Pax2-Cre N-Myc f/f* mice, the horizontal canal was absent; but, neither the anterior nor posterior canals were noted to be distorted (Kopecky et al., 2011). Here, in the dCKO mice, in addition to the absence of horizontal canal, the anterior canal was always found to be affected. The anterior canal appeared much thinner with an impartially reabsorbed segment. In summary, the *L-Myc* CKO mice had no noticeable variation from control littermates, the *N-Myc* CKO mice had an identical phenotype to the *Pax2-Cre N-Myc f/f* mice and the dCKO mice had the most severe defects.

In addition to assessing overall morphogenetic changes, three dimensional reconstructions allowed quantification of inner ear endolymphatic space changes (Fig. 2). Overall there was minimal endolymphatic space change in early development despite the vast morphological changes and overall growth of the control inner ear (Fig. 1). After E15.5 the endolymphatic space greatly increased coinciding with the formation of the ductus reuniens and utriculosaccular foramen (Fig. 2). Similar findings were noted in the *L-Myc* CKO ears that were nearly identical to control with minimal change until after E13.5 and increased after E15.5. These values were consistent between the confocal based three dimensional reconstructions and previous reconstructions using sTSLIM (Kopecky et al., 2012b). However, while compared between the *N-Myc* CKO and the control, a noticeable decrease in endolymphatic space was observed at each time points starting from E10.5 to E18.5 (Fig. 2). Despite the reduction in volume in the *N-Myc* CKO mice, there was little endolymphatic space increased after E15.5 which remained reduced compared to control littermate (Fig. 2). Lastly, we quantified the volumetric changes that occurred in the dCKO ears. The overall endolymphatic space in the dCKO ears was significantly decreased ($p < 0.05$) compared to both control and *L-Myc* CKO ears during the entire embryonic development (Fig. 2). It was also reduced in comparison to the *N-Myc* CKO ears (Fig. 2). Therefore, it is obvious that the loss of *L-Myc* alone had minimal effect on overall morphogenesis of the ear; however, the loss of *L-Myc* in combination with *N-Myc* produced a greater effect than the loss of *N-Myc* alone.

Consistent with the pattern of the other mutant ears, there was minimal change in endolymphatic space until E15.5 in dCKO ears which after E15.5 had increased but the relative ratio remained reduced compared to control. Interestingly, in all of the four mice, endolymphatic space began to increase at the same time, suggesting that this increase is unrelated to the loss of *N-Myc* or *L-Myc* and is not dependent upon the proper formation of the inner ear, rather most notably on the formation of the ductus reuniens and utriculosaccular foramen.

N-Myc is More Important than *L-Myc* for the Formation and Functionality of the Inner Ear

At P0, all areas expressing *Pax2* (inner ear, kidneys, and cerebellum) were substantially reduced in size in both the *N-Myc* CKO and dCKO mice compared to the *L-Myc* CKO mice which itself showed only a small reduction in size compared to control (Fig. 3). Areas not expressing *Pax2*, such as the forebrains, were not reduced in size in any of the mice. In addition to the added size reductions, the dCKO mice were 100% lethal shortly after birth whereas some *N-Myc* CKO and all control and *L-Myc* CKO mice were viable. The reason why all the dCKO mice die is unclear but indicates a crucial compounding effect that likely is compensated for by either of the *Myc* transcription factors in the single knockout mice.

There were a number of defects observed while comparing the control and the dCKO mice. Most importantly, the cochlea was abnormally formed, notably the extreme base and apex were affected most (compare Fig. 4A and 4D). The base lost its high frequency hook region (compare Fig. 4A' and 4D') and the apex was truncated and contained a ball-like formation of cells (compare Fig. 4A'' and 4D'') as shown with the three dimensional reconstructions. Recognizable hair cells were found in newborn dCKO shown with Myo7a immunohistochemistry (Fig. 4B, B', F, F'). Similar to the *Pax2-Cre N-Myc f/f* mice (Dominguez-Frutos et al., 2011; Kopecky et al., 2011), the dCKO mice had a fusion of the utricle and saccule as well as a partial fusion or abnormal tapering of the base of the cochlea (compare Fig. 4B' and 4F'). The sections from the apex of the dCKO mice revealed a vestibular-like sensory epithelium sitting on periotic mesenchyme with a uniform set of vestibular-like hair cells (Fig. 4C, C', E–E"). The hair cells at the most apical tip resembled type 1 and type 2 vestibular hair cells (black arrow in Fig. 4E and 4E') and those closer to the middle turn resembled more cochlear type hair cells (white arrow in Fig. 4E, and 4E''') and sat on periotic space comparable to a scala tympani.

While dCKO mice were lethal shortly after birth precluding behavioral studies, three *N-Myc* CKO mice survived up to P21 and were assessed for long-term functionality of remaining hair cells using auditory brainstem response (ABR). No responses could be elicited upon administration of the click stimuli or at any frequency tested (data not shown) consistent with *Pax2-Cre N-Myc f/f* mice previously described (Kopecky et al., 2012a). However, when quantifying the same parameters for the *L-Myc* CKO mice (Fig. 5A), statistically significant differences ($p<0.05$) were noted in almost all ABR responses (except at 24kHz and 28kHz). Behavioral gait performance was implemented using the Noldus Catwalk System to assess vestibulo-motor performance (a combined function of inner ear and cerebellum) through a number of gait performance assessments. Specifically for gait performance, we measure regularity which quantitatively accounts for how consistently a mouse walks within a normal footfall pattern as we previously described (Kopecky et al., 2012a). While there were no gross morphological defect, the *L-Myc* CKO mice has significantly lower gait regularity compared to control littermate ($p<0.015$; Fig. 5B). Three *N-Myc* CKO mice were also used for the gait performance assessment but these mice were unable to walk in the Catwalk system due to severe ataxia (data not shown). The *N-Myc* CKO mice contrasted with the *L-Myc* CKO mice as *N-Myc* CKO mice had severely disrupted hearing (no response) and balance (ataxic) consistent with their noted abnormalities (Kopecky et al., 2012a), whereas *L-Myc* CKO mice had some defect in both hearing and gait (Fig. 5) despite their near normal development (Fig. 1–3).

Proliferation is Severely Truncated after the Loss of both *N-Myc* and *L-Myc*

In both the *N-Myc* CKO and dCKO mice, the growth of the entire inner ear was stunted with abnormal neurosensory differentiation (Fig. 1–3). The dCKO mice were not viable past P0, but the P21 *N-Myc* CKO were viable but were completely deaf despite initial formation of hair cells, consistent with previous data showing the loss of inner ear cochlear hair cells after P14 in the absence of early embryonic expression of *N-Myc* (Kopecky et al., 2011; Kopecky et al., 2012a). We have shown that this loss was not a result of late-onset effects of *N-Myc* or *L-Myc* (Kopecky et al., 2012c) and must be due to an early insult, possibly due to a disruption in the timing between proliferation and differentiation. To this end, proliferation was assessed at E13.5 with the thymidine analog 5'-Ethynyl-2'-deoxyuridine (EdU) which was injected into pregnant dams eight hours prior to sacrifice. At E13.5, cells at approximately 15% of the distance from the extreme base toward the apex (termed "base") along the presumptive organ of Corti were assessed for proliferation markers EdU as well as CyclinD1. In the control, EdU (Fig. 6A) and CyclinD1 (Fig. 6B) were seen throughout the entire basal region. At approximately 50% of the distance from base to apex (termed

"middle"), EdU (Fig. 6C) and CyclinD1 (Fig. 6D) were seen only in the more basal portion of the middle turn whereas cells showed no signs of proliferation towards the apex. This suggested that in the control cochlea, organ of Corti precursor cells continued proliferating in the base and reduced in the middle, but not in the apex. This was consistent with apical cell cycle exit at E12.5, middle turn cell cycle exit at E13.5, and basal cell cycle exit at E14.5 (Matei et al, 2005). On the other hand, in the dCKO mice, EdU (Fig. 6E, G) and CyclinD1 (Fig. 6F, H) were seen only in the base which was severely reduced and were absent in the middle turn compared to control. This showed that at E13.5, only cells in the base are continuing proliferation whereas cells in the middle turn and apex have likely exited the cell cycle (Fig. 6). Together, it appeared that in the absence of both *N-Myc* and *L-Myc*, organ of Corti cells exited the cell cycle approximately one day earlier than control organ of Corti cells.

In the Absence of *N-Myc* and *L-Myc,* Numerous Molecular Pathways are affected: Including Differentiation and Cell Maintenance Genes *Neurod1, Atoh1, Pou4f3*, and *Barhl1*

Reduction in proliferation-associated genes in absence of both N-Myc and L-Myc—Proliferation in the inner ear is driven in part by *N-Myc* and *L-Myc* whereas differentiation of neurons and hair cells are a result of *Neurod1* and *Atoh1* upregulation, respectively, and the hair cell sub-types are fine-tuned by the interaction of these transcription factors (Jahan et al., 2010). Both *N-Myc* and *L-Myc* potentially regulate the timing of differentiation through two interdependent mechanisms, cell cycle regulation and inhibition of differentiation. We assessed molecular changes in various genes of both of these pathways in the absence of *Myc* at E11.5 through E15.5 and at P0. In dCKO mice, *N-Myc* and *L-Myc* mRNA levels were drastically reduced as shown through qRT-PCR. In their absence, *pRb, E2F4*, and $p27^{Kip1}$ (Table 1) were also reduced. Interestingly, *CyclinD2* and *E2F2* showed minimal change (Table 1). However, *Id* 2–*3*, which interact with bHLH class II E-proteins such as *Atoh1* and *Neurod1,* were affected, with *Id2* showing the greatest downregulation while *Id3* was nearly unaffected (Table 1).

Timing of differentiation and maintenance genes are disrupted by altered proliferation—The qRT-PCR data from E11.5 to P0 mice revealed that *Neurod1* mRNA levels were reduced in dCKO mice compared to control littermates (Table 1). *Atoh1* mRNA levels in dCKO mice were notably reduced from E12.5 through E15.5 compared to control; however, at E14.5 and E15.5, *Atoh1* levels in dCKO increased but never reached to control limits, suggesting a delayed and partial upregulation in the absence of *N-Myc* and *L-Myc*. At P0, *Atoh1* levels were minimally reduced (Table 1). These qRT-PCR expression data of *Atoh1* mRNA levels were validated through *in situ* hybridization (Fig. 7). At E13.5, no *Atoh1 in situ* expression was detected in the dCKO mice (Fig. 7B) whereas it was strongly expressed in the vestibular system in control (Fig. 7A). At E14.5, *Atoh1* is expressed throughout the vestibular epithelia as well as in the basal-middle turn and extending towards the apex in the control (Fig. 7C). *Atoh1* was restricted only in the vestibular epithelia in the E14.5 dCKO littermates (Fig. 7D), suggesting about a one day delay in *Atoh1* upregulation. At P0, *Atoh1* was expressed in all sensory epithelia including the cochlea in both control (Fig. 7E) and dCKO (Fig. 7F). Downstream hair cell maintenance genes of *Atoh1* include *Pou4f3* and *Barhl1*, were reduced in the dCKO mice detected by qRT-PCR (Table 1). A number of other organ of Corti specifying and defining genes were likewise downregulated, including *Fgf8, Pax2, Gata3*, and *Sox2* (Table 1).

Summary of control and *Pax2-Cre N-Myc L-Myc* Mutant Mice

Pax2-Cre N-Myc f/+ L-Myc f/+ mice were crossed with *N-Myc f/f L-Myc f/f* mice to assess functional redundancy of *N-Myc* and *L-Myc* and to help elucidate the potential mechanism behind initial hair cell formation followed by subsequent loss initially described in *Pax2-Cre*

N-Myc f/f mice. In the absence of *L-Myc, N-Myc* appeared to be able to nearly fully compensate as *L-Myc* CKO mice developed normally with no apparent morphologic or neurosensory defects; however, these mice performed worse when assessed for hearing and balance performance, suggesting an incomplete ability of *N-Myc* to compensate for *L-Myc* loss. In the absence of *N-Myc, L-Myc* was unable to compensate for the loss as inner ears were severely reduced in size, with morphologic abnormalities, and viable mice could not hear. In the absence of both *N-Myc* and *L-Myc*, inner ears were more severely affected with a further reduction in endolymphatic space, additional cochlear and vestibular defects, and a 100% lethality rate shortly after birth. These dCKO mice stopped noticeable cell division in the middle turn of the cochlea around E13.5, approximately one full day earlier than control mice (Fig. 6, 8). This premature cell cycle exit resulted in approximately one day delay in *Atoh1* upregulation (Fig. 7, 8). Altered proliferation and differentiation resulted from the dramatic reduction in mRNA levels of *N-Myc* and *L-Myc* which correlated with the altered timing and expression levels of *Neurod1* and *Atoh1*, possibly through interaction with the *IDs* (Table1). These altered levels of *Atoh1* corresponded with reduced levels of cell maintenance genes *Pou4f3* and *Barhl1*. The apparent transformation of the apical tip into an almost vestibular macula-like epithelium and the complete loss of the basal hook region indicate that it is in particular the start and the stop of the organ of Corti hair cell formation that is affected by the absence of *Myc* signaling.

Discussion

N-Myc can Partially Compensate for the Loss of *L-Myc* whereas *L-Myc* cannot Compensate for *N-Myc* Loss

Both *N-Myc* and *L-Myc* are co-expressed strongly in the inner ear, with both detectable by E8.5 (Dominguez-Frutos et al., 2011; Kopecky et al., 2011). The expression domains of *N-Myc* and *L-Myc* mostly overlap, suggesting that there is possible redundancy between the two ear expressed *Mycs*. By crossing *Pax2-Cre N-Myc f/+ L-Myc f/+* with *N-Myc f/f L-Myc f/f*, four unique phenotypes are generated, a control, one that knocked out *L-Myc* completely, one that knocked out *N-Myc* completely, and one that knocked out both. In assessing the *L-Myc* knockouts, there seems to be no obvious morphologic abnormalities as these mice developed nearly identically to control, even if combined with *N-Myc* heterozygosity (Fig. 1). However, in the absence of *L-Myc* in *Pax2* expressing regions at P0, the inner ear, kidney, and cerebellum are slightly reduced in size. Furthermore, functional studies of *L-Myc* CKO mice at P21 showed a slight reduction in auditory and vestibular functioning (Fig. 5). In contrast, *N-Myc* CKO mice have severe morphologic abnormalities throughout development, are reduced in size, and have a complete loss of hearing. While these abnormalities are worse in the absence of both *N-Myc* and *L-Myc*, it is obvious that the loss of *L-Myc* alone has only minimal effect on overall development and functionality whereas loss of *N-Myc* greatly alters the formation of the inner ear. Thus, *N-Myc* appears to play a much more pervasive role in inner ear development whereas *L-Myc* seems to play only an auxiliary function that can be mostly overcome through *N-Myc* expression. The neonatal death of the dCKO mice indicates that certain crucial aspects of development are non-redundant suggesting a limited but essential function of *L-Myc* that remains to be determined as it likely is masked by *N-Myc* as long as this gene is normally expressed.

Proper Timing and Expression Levels of bHLH Transcription Factors Necessary for Differentiation are Dependent on Proliferation

The roles of the *Mycs* throughout the body and their interactive cascades regulating proliferation is ancient (Young et al., 2011) and has been well-studied (Conacci-Sorrell and Eisenman, 2011). However, the *Mycs* have been minimally studied in the inner ear and this is the first study attempting to elucidate the molecular networks involved with *Myc*

signaling in the inner ear. Importantly, our data suggest that the alteration of proliferation through the *Myc's* leads to disruption of cellular differentiation. In the absence of *N-Myc* and *L-Myc*, proliferation is greatly reduced and downstream *Id2* and CyclinD1 are also reduced. Contrary to initial expectations, while this downregulation of *Id2* may lead to a disinhibition of class II bHLH transcription factors (Fritzsch et al., 2006), such an effect would be compromised due to the downregulation of both *Neurod1* and *Atoh1* expression. *Neurod1* is expressed as early as E9.5 in the otic vesicle but is restricted to the vestibulo-cochlear ganglion by E10.5 and is essential for differentiation of neurons and interacts with *Atoh1*, necessary for hair cell formation (Jahan et al., 2010). *Neurod1* levels never reached control levels in the dCKO mice. *Atoh1*, which is necessary for hair cell differentiation and forms a feedback loop with *Neurog1* (Bermingham et al., 1999; Matei et al., 2005; Raft et al., 2007; Kirjavainen et al., 2008; Pan et al., 2011), is downregulated until E13.5 in dCKO mice after which *Atoh1* slightly increases but remains below control levels. This transient downregulation of *Atoh1* coincides with decreased levels of downstream hair cell maintenance genes *Pou4f3* and *Barhl1*. *Pou4f3* (Xiang et al., 2003; Clough et al., 2004; Chellappa et al., 2008; Masuda et al., 2012) and *Barhl1* (Chellappa et al., 2008) are both well-known to play roles in long-term hair cell maintenance (Pauley et al., 2008). It has been previously shown that level and timing of *Atoh1* (Jahan et al., 2010; Pan et al., 2012) and expression of *Pou4f3* and *Barhl1* are all necessary for proper hair cell formation and long-term maintenance. The *Pou4f3* promoter region is only partially characterized but is known to contain multiple binding sites including several E-boxes (Masuda et al., 2011). While we cannot say with certainty whether the progressive hair cell loss after initial hair cell formation is due to the delayed *Atoh1* upregulation or the subsequent reduction of *Pou4f3* and *Barhl1*, it is clear that by altering *N-Myc* and *L-Myc*, molecular pathways initiating and maintaining differentiation are disrupted, showing that in the ear, proliferation and differentiation are interconnected, at minimum through the *Myc* node, possibly by limiting the expression levels of *Pou4f3* and *Barhl1* expression, both crucial genes for long-term hair cell maintenance. Compounding cochlear hair cell death could also be the potential disruption of endocochlear potential (Cable et al., 1993; Tran, 2002) resulting from the failure of the ductus reuniens forming. It is conceivable that this results in a change in endocochlear potential to approximate the vestibular endopotential, potentiating hair cell loss.

N-Myc and *L-Myc* Regulate the Development of the Inner Ear through a Partially Understood Molecular Network

In the absence of *N-Myc* and *L-Myc*, a number of abnormalities result as the end-product of inner ear development, two of which are a reduction in proliferation and a progressive loss of hair cells; these abnormalities likely are related to the interaction between proliferation and differentiation. However, a much more complicated picture arises when the remainder of the morphologic and neurosensory abnormalities associated with the dCKO mice is considered. Beyond the issue of long-term viability, the reduction of high frequency end of basal 'hook' region in the cochlea and the transformation of the apex into an unusual organization with hair cells of a mixed vestibular/cochlear phenotype indicate that the *Myc* bHLH transcription factors are likely affecting not only proliferation but also play into the cell fate decision making process, possibly through interfering with *Atoh1* signaling, the only other gene known to affect directly hair cell type differentiation (Jahan et al., 2010).

Alternatively, the truncated development may lead to altered interaction of proliferating/postmitotic cells that result in the observed changes on the basal and apical part of the organ of Corti. To sort out the possible mechanisms by which some of these defects arose, we assessed several candidate genes. *Fgf8* is expressed in the prospective otic placode by E8 and in the ventral otic placode by E9 and is important for the induction of the otic placode as

its loss results in abnormal otic placode morphology (Ladher et al., 2005; Hertzano et al., 2010). It is later expressed in inner hair cells (Jacques et al., 2007; Jahan et al., 2010; Jahan et al., 2012). *Fgf8* is progressively downregulated in the dCKO shown by the qRT-PCR data (Table 1) as well as previously with *in situ* hybridization in *Pax2-Cre N-Myc f/f* mice (Kopecky et al., 2011). Another gene, *Pax2* is expressed by E8.5 in the otic placode and in the medial sensory and non-sensory components of the cochlea at birth. *Pax2* initially defines the pre-otic field and is induced by *Fgf* signaling and is dependent on *Shh* (Riccomagno et al., 2005; Bouchard et al., 2010). The dCKO mice have greatly reduced levels of *Pax2*. Another gene early expressed in the otic placode is *Gata3* and in its absence, the otocyst remains cystic (Karis et al., 2001; Duncan et al., 2011). In the absence of *N-Myc* and *L-Myc, Gata3* is downregulated. Another gene, *Sox2* is expressed in the ventral neural region at E9.5 and later in hair cells and supporting cells of the cochlea (Dabdoub et al., 2008; Nichols et al., 2008). *Sox2* mutants do not form a defined prosensory domain and have disorganization of hair cells. *Sox2* inhibits *Atoh1* expression but promotes *Prox1* expression (Kiernan et al., 2005; Dabdoub et al., 2008; Mak et al., 2009). In the absence of *N-Myc* and *L-Myc, Sox2* is also downregulated indicating alterations in the fate determination of sensory epithelia. These data suggest that prosensory specification is changed as a direct consequence in the absence of *Myc* TFs. Future work needs to establish the interaction of *Mycs* on the promoter regions of these various factors to provide a rational basis how the observed molecular changes tie into the obvious morphological changes. Additionally, while this appears to be a cell autonomous effect, conclusive findings may require the use of inducible *Cre* lines or at minimum a ubiquitously expressed *Cre* to test how the timing of *Myc* deletion affects expression of these genes. However, targeted inducible lines with exclusive ear expression are not yet available and ubiquitously expressed lines such as Ros26ER-Cre may themselves have confounding effects due to widespread deletion of *Mycs* and a likely limited viability.

Mycs are Necessary for the Formation of Therian Novelties in the Cochlea

Comparative data shows that among tetrapods, only therians have high frequency hearing above 10kHz in the hook region (Muller et al., 2005) and have lost the lagena at the apical tip of the cochlear duct, instead show a coiled cochlea (Webster et al., 1992; Fritzsch et al., 2011; Duncan and Fritzsch, 2012). Our data suggests that *Myc* mediated proliferation and hair cell fate regulation may play a role in this evolutionary process. Clearly, the premature termination of proliferation in dCKO mice result in a complete loss of the basal hook region, the high frequency mapping part, unique to the therian organ of Corti. Likewise, there is vestibular-like transformation at the apical tip of the shortened cochlear duct that has multiple hair cells sitting on top of periotic mesenchyme, typical for vestibular maculae, instead of a periotic space which is an essential feature of the organ of Corti. Interestingly, disassociation of the scala tympani leads a vestibular-like basal turn in the *Lmx1a* mutant (Nichols et al., 2008), similar to what apparently occurs in the apex in the dCKO mice. Data are now needed to establish the evolutionary recruitment of the *Mycs* to the growing cochlea, which likely happened in the therian ancestor after their split from monotremes that lack both the high frequency reception (Fay, 1988) and retain the ancestral lagenar macula at the tip of their cochlear duct (Fritzsch, 1987; Jorgensen and Locket, 1995).

Conclusions

N-Myc and *L-Myc* are mostly co-expressed in the inner ear. The early conditional embryonic loss of both genes using *Pax2-Cre* results in a severely disrupted ear representing a more profound phenotype compared to the loss of *N-Myc* alone. The combined losses of both *N-Myc* and *L-Myc* not only reduces proliferation and growth of the ear but also leads to subsequent alteration of differentiation, most notably through the reduction and delay of

Atoh1 and downstream hair cell maintenance factors *Pou4f3* and *Barhl1*. Morphologic changes are most striking in the base and the apex of the developing cochlea. Importantly, the loss of *L-Myc* alone has minimal effect on inner ear development suggesting a greater importance of *N-Myc* in mammalian inner ear development. The current study in conjunction with previously published studies detailing *N-Myc* and *L-Myc* in the inner ear illustrates the importance of proliferation control to proper neurosensory differentiation early in development. Any attempt to form hair cells, regardless of precursor source, may ultimately need to account for the interaction of proliferation genes such as the *Mycs* with differentiation genes such as *Atoh1* and possibly other upstream genes such as *Eya1* and *Six1*. Increased efforts should be made to more fully elucidate the molecular networks balancing these two interdependent processes for a therapeutically safe application in organ of Corti reconstitution.

Experimental Procedures

Mice and genotyping

A double conditional knockout line was generated by combining *Pax2-Cre* mice (Ohyama and Groves, 2004) with *N-Myc* floxed mice (Jackson Labs B6.129-*N-Myc*^{tm1Psk}/J) and *L-Myc* floxed mice (donated by Dr. Eisenman). Tail biopsies were used for genomic DNA and polymerase chain reactions for genotyping were performed using the following primers (*N-Myc:* IMR6727 5’gtcgcgctagtaagagctgagatc 3’ IMR6729 5’ cacagctctggaaggtgggagaaagttgagcgtctcc 3’ *Cre:* 1 5’ cctgttttgcacgttcaccg 3’ 2 5’ atgcttctgtccgtttgccg 3’ IMR42 5’ ctaggccacagaattgaaagatct 3’ IMR43 5’ gtaggtggaaattctagcatcatcc 3’). Animal care and usage was in accordance with the approved University of Iowa Institutional Animal Care and Use Committee (IACUC) guidelines for the use of laboratory animals in biological research (ACURF # 0804066 and 1103057).

Noldus Catwalk

The Noldus Catwalk System ® consists of a walkway floor containing a sheet of glass encased with a light. P21 mice were placed in a corridor 60cm long by 10cm wide and allowed to move freely. A mounted camera captured a 40cm × 10cm field from below the walkway. As the mouse entered the field of view, a run was initiated and stored on a computer. If the mouse exited the field of view within 10 seconds and there was less than a 60% variation in speed, the run was compliant. Numerous compliant runs were acquired for each mouse and were termed a trial. Between each trial, the walkway barrier was removed and the glass was cleaned using standard glass cleaner. All mice were tested under similar conditions. After each trial, the acquired data was classified. Classification is the semi-automated process of entering which limb induced the recorded print. Data points for each mouse are an average of three compliant runs. The catwalk system has many gait performance parameters. Regularity measures the “normalcy” of gait and how consistent the contralateral limbs are in contact with the glass walkway.

Auditory Brainstem Response (ABR)

Mice were anesthetized with 0.025mL/g of the anesthetic Tribromoethanol (*Avertin*®) and after a surgical level of anesthesia was induced, needle electrodes were inserted subcutaneously in the vertex, slightly posterior to the pinna, and in the contralateral hind-limb. A speaker was placed 10cm from the pinna of the left ear and computer-generated stimuli were given in an open field environment in a soundproofed chamber. Clicks were presented and responses were averaged across 512 presentations using Tucker-Davis Technologies System hardware running BioSig® Software. Recorded signals were band-pass and notch-filtered (300Hz–5kHz, 60Hz). The sound level was decreased in 3dB steps from a 96dB sound pressure level until there was no noticeable response. Identical set-up but

a tone pip program was given from 2kHz through 28kHz incrementally with a stepwise decrease in amplitude at each frequency.

Perfusion

Mice were injected intraperitoneally (IP) with greater than a 0.025mL/g of the anesthetic Tribromoethanol (*Avertin*®) and after ocular and pedal reflexes ceased, 4% paraformaldehyde (PFA) was pumped continuously with a 30-gauge needle into the left ventricle. The right atrium was opened to facilitate clearing. After fixation, heads were hemi-dissected, placed in 4% PFA in a multiwell plate, and covered with parafilm for long-term storage.

Epoxy Resin Sections

Dissected ears were incubated for two hours with 2.5% glutaraldehyde and washed with 0.1M phosphate buffer three times over a period of two hours. Ears were reacted in 1% osmium tetroxide for approximately one hour, or until tissue was dark, and rinsed with 0.1M phosphate buffer. Samples were dehydrated with an ascending graded ethanol series and then incubated with a 1:1 100% ethanol and propylene oxide mixture. Samples were mixed with Epon 812 and propylene oxide overnight and then oriented and embedded with Epon 812 and placed in an incubator for twenty-four hours at 60°C. Ears were sectioned at 1μm with a Leica Ultratome and sections were retrieved from water bath and placed on heated slides in sequential order. They were allowed to bake onto the glass slide and stained for one minute with Stevenel's Blue and imaged. Stained slides were rinsed with dH_20 and allowed to dry. Sections were coverslipped using DMX mounting solution and allowed to dry overnight. Samples were imaged with Nikon Eclipse 800 microscope and captured with Image-Pro.

EdU Staining

Pregnant dams were injected intraperitoneally with 100μg EdU/gram body weight of mouse. After 8 hours, the mothers were sacrificed and pups were fixed and stored in 4% PFA. Dissected ears were then reacted with Click-iT reaction cocktail according to manufacturer's instructions (Invitrogen C35002).

Immunohistochemistry

Ears were dissected in 0.4% PFA and defatted overnight in 70% ethanol. They were removed from ethanol and blocked for two hours in blocking solution [(5% normal goat serum, 0.1% Triton X-100, in Phosphate buffered saline (PBS)]. Myo7a (1:200; Proteus Biosciences, 25-6790) and CyclinD1 (1:200; Thermo Scientific, RM-9104) were diluted in the blocking solution and incubated for three days at 4°C on a shaker. Ears were washed with PBS three times for two hours each and Alexa Fluor 633 anti-mouse or anti-rabbit secondary antibodies were diluted in blocking buffer and incubated for two days, covered with aluminum foil, in 4°C. Ears were incubated in were rinsed in PBS and mounted on a glass-slide in glycerol. Images were captured with the TCS SP5 multiphoton confocal microscope.

Three Dimensional Reconstruction

Tissue Preparation—Ears were decalcified in 10% EDTA for four days with fresh EDTA changed daily. Ears were rinsed with PBS at least three times with each wash lasting about two hours. Ears were put into 70% EtOH overnight. Ears were at this point put in 100% EtOH for two hours and then placed two days in a 100% rhodamine isothiocyanate and EtOH mixture until tissue was very lightly stained. 100% rhodamine EtOH mixtures were removed and clearing solution was added to 100% EtOH to obtain a 1:1 ratio. Clearing

solution was made with five parts methyl salicylate to three parts benzyl benzoate (MSBB). The 1:1 100% EtOH to MSBB was replaced with 100% MSBB overnight at room temperature. Ears were then put in two changes of MSBB and imaged.

Confocal Imaging—Ears were placed on a glass slide and Dow Corning Grease was applied to the glass slide to make a retainer for MSBB. Ears were placed in the MSBB bath and spacers were added to ensure absence of compression stresses after coverslip application. Using a TCS SP5 confocal microscope, Z-stacks of three to five micron increments were obtained.

Segmentation and three dimensional renderings—Z-stacks were loaded into Amira Version 5.4. All endolymphatic spaces were segmented in each section. Segmented images were resampled (2×2×1), surface generated (unconstrained), smoothed (20 iterations), and the surface was viewed. Quantitative measurements were obtained through the three dimensional measurement functions within the Amira software. Protocol can now be viewed in full detail (Kopecky et al., 2012d).

qRT-PCR

Embryos from E11.5 through E15.5 were retrieved from the uterus in an RNAse free environment. Embryos were placed into RNAlater for storage. P0 pup ears were immediately dissected and placed into RNAlater. RNAlater fixed inner ears were then dissected in RNAlater and homogenized and RNA was extracted using the Qiagen RNeasy Plus Mini Kit (Qiagen; Valencia, CA) followed by cDNA synthesis with Invitrogen Super Script III. Due to the inability to dissect out sensory epithelia from the inner ear at E11.5, we used the entire inner ear for all ages (a dissected ear using only sensory epithelia later would provide biased results from earlier entire ears). cDNA was then mixed with a master mix consisting of Roche Master Mix, water, a Roche Universal Probe Library Probe designed as intron spanning from the Roche Website (https://www.roche-applied-science.com/sis/rtpcr/upl/index.jsp?id=UP030000), and primer pairs (from Integrated DNA Technologies, IDT). All primer pairs and probes were verified with serial RNA dilutions with standard curves created to assess reverse transcription inhibition. Similar dilutions were performed with cDNA to quantify the minimal concentration of cDNA for each reaction. 96-well plates with three technical replicates were run on the Roche Light Cycler 480 housed in the Carver Center for Genomics at the University of Iowa. For each recorded gene and time point, at least three biological replicates were run following the established MIQE protocol (Bustin et al., 2009). Statistical analysis of qRT-PCR data was performed through either the Roche Light Cycler 480 SW 1.5 software or through Microsoft Excel. Fold change was calculated by normalizing the difference of target Cp values to reference Cp values of both positive control and unknown. For student t-Tests, statistical significance was set at the 0.05 level unless indicated otherwise.

In situ Hybridization

In situ hybridization was performed using the *Atoh1* anti-sense RNA probe (provided by Huda Y. Zoghbi) labeled with digoxigenin. The plasmids containing the cDNAs were used to generate the RNA probe by *in vitro* transcription. Mice were perfused and fixed in 4% PFA after anaesthetized with Avertin. The ears were dissected in 0.4% PFA and dehydrated and rehydrated in graded methanol series and then digested briefly with 20 μg/ml of Proteinase K (Ambion, Austin, TX, USA) for 15–20 minutes according to the stages of the mice. Then the samples were hybridized overnight at 60°C to the riboprobe in hybridization solution containing 50% (v/v) formamide, 50% (v/v) 2X saline sodium citrate (Roche) and 6% (w/v) dextran sulphate. After washing off the unbound probe, the samples were incubated overnight with an anti-digoxigenin antibody (Roche Diagnostics GmbH,

Mannheim, Germany) conjugated with alkaline phosphatase. After a series of washes, the samples were reacted with nitroblue phosphate/ 5-bromo, 4-chloro, 3-indolil phosphate (BM purple substrate, Roche Diagnostics, Germany) which is enzymatically converted to a purple colored product. The ears were mounted flat in glycerol and viewed in a Nikon Eclipse 800 microscope using differential interference contrast microscopy and images were captured with Metamorph software.

Area measurements

Heads were hemisected and ears removed from the head. Lateral images of the ear were taken and width (anterior to posterior) and height (ventral to dorsal) measurements were acquired. Cerebellum cross sectional area from the hemisected head was also measured identical to the inner ear. The forebrain was measured from the hemisected head and the cross sectional area of the midline was measured. Lastly, kidneys were removed from the retroperitoneal space and cross sectional height from inferior to superior pole and width from medial to lateral were assessed.

Acknowledgments

We would like to thank Dr. Peter Santi and his lab, notably Shane Johnson and Heather Schmitz for their assistance in developing the protocol for sTSLIM image processing which we adapted for confocal imaging as well as their guidance in Amira usage. We thank Dr. Thomas Schimmang and his lab for their helpful discussions of the *Pax2-Cre N-Myc* CKO mice. We would like to thank Drs. T. Ohyama and A. Groves for providing the Tg(*Pax2-Cre*) line. We thank Jackson Lab for providing the *N-Myc f/f* mice and Dr. Knoepfler for donating them. We would also like to thank Dr. Eisenman for donating the *L-Myc f/f* mice. The Leica TCS SP5 confocal microscope was purchased in part with a grant from the Roy J. Carver foundation. Grant funding for Bernd Fritzsch was provided through the NIH and NIDCD R01-DC055095590. Funding for Benjamin Kopecky was provided by the CTSA, grant number UL1RR024979. We thank the NIH P30 grant (DC010362) to make the ABR equipment and the Noldus Catwalk System available as part of the supported core facilities. We thank the University of Iowa Carver College of Medicine, Medical Scientist Training Program, and Office of the Vice President for Research for support.

Grant Funding: NIDCD R01-DC055095590 (BF), CTSA UL1RR024979 (BK), NIH P30-DC010362

References

Ahmed M, Wong EY, Sun J, Xu J, Wang F, Xu PX. Eya1-Six1 interaction is sufficient to induce hair cell fate in the cochlea by activating Atoh1 expression in cooperation with Sox2. Dev Cell. 2012a; 22:377–390. [PubMed: 22340499]

Ahmed M, Xu J, Xu PX. EYA1 and SIX1 drive the neuronal developmental program in cooperation with the SWI/SNF chromatin-remodeling complex and SOX2 in the mammalian inner ear. Development. 2012b

Bent T, Buchwald A, Pisoni DB. Perceptual adaptation and intelligibility of multiple talkers for two types of degraded speech. J Acoust Soc Am. 2009; 126:2660–2669. [PubMed: 19894843]

Bermingham NA, Hassan BA, Price SD, Vollrath MA, Ben-Arie N, Eatock RA, Bellen HJ, Lysakowski A, Zoghbi HY. Math1: an essential gene for the generation of inner ear hair cells. Science. 1999; 284:1837–1841. [PubMed: 10364557]

Bhattacharya A, Baker NE. A network of broadly expressed HLH genes regulates tissue-specific cell fates. Cell. 2011; 147:881–892. [PubMed: 22078884]

Bouchard M, de Caprona D, Busslinger M, Xu P, Fritzsch B. Pax2 and Pax8 cooperate in mouse inner ear morphogenesis and innervation. BMC Dev Biol. 2010; 10:89. [PubMed: 20727173]

Bustin SA, Benes V, Garson JA, Hellemans J, Huggett J, Kubista M, Mueller R, Nolan T, Pfaffl MW, Shipley GL, Vandesompele J, Wittwer CT. The MIQE guidelines: minimum information for publication of quantitative real-time PCR experiments. Clin Chem. 2009; 55:611–622. [PubMed: 19246619]

Cable J, Jackson IJ, Steel KP. Light (Blt), a mutation that causes melanocyte death, affects stria vascularis function in the mouse inner ear. Pigment Cell Res. 1993; 6:215–225. [PubMed: 8248019]

Chang YP, Fu QJ. Effects of talker variability on vowel recognition in cochlear implants. J Speech Lang Hear Res. 2006; 49:1331–1341. [PubMed: 17197499]

Chellappa R, Li S, Pauley S, Jahan I, Jin K, Xiang M. Barhl1 regulatory sequences required for cell-specific gene expression and autoregulation in the inner ear and central nervous system. Mol Cell Biol. 2008; 28:1905–1914. [PubMed: 18212062]

Chen P, Johnson JE, Zoghbi HY, Segil N. The role of Math1 in inner ear development: Uncoupling the establishment of the sensory primordium from hair cell fate determination. Development. 2002; 129:2495–2505. [PubMed: 11973280]

Chen P, Zindy F, Abdala C, Liu F, Li X, Roussel MF, Segil N. Progressive hearing loss in mice lacking the cyclin-dependent kinase inhibitor Ink4d. Nat Cell Biol. 2003; 5:422–426. [PubMed: 12717441]

Clough RL, Sud R, Davis-Silberman N, Hertzano R, Avraham KB, Holley M, Dawson SJ. Brn-3c (POU4F3) regulates BDNF and NT-3 promoter activity. Biochem Biophys Res Commun. 2004; 324:372–381. [PubMed: 15465029]

Colletti L, Mandala M, Zoccante L, Shannon RV, Colletti V. Infants versus older children fitted with cochlear implants: Performance over 10 years. Int J Pediatr Otorhinolaryngol. 2011

Conacci-Sorrell M, Eisenman RN. Post-translational control of Myc function during differentiation. Cell Cycle. 2011; 10:604–610. [PubMed: 21293188]

Dabdoub A, Puligilla C, Jones JM, Fritzsch B, Cheah KS, Pevny LH, Kelley MW. Sox2 signaling in prosensory domain specification and subsequent hair cell differentiation in the developing cochlea. Proc Natl Acad Sci U S A. 2008; 105:18396–18401. [PubMed: 19011097]

Dominguez-Frutos E, Lopez-Hernandez I, Vendrell V, Neves J, Gallozzi M, Gutsche K, Quintana L, Sharpe J, Knoepfler PS, Eisenman RN, Trumpp A, Giraldez F, Schimmang T. N-myc controls proliferation, morphogenesis, and patterning of the inner ear. J Neurosci. 2011; 31:7178–7189. [PubMed: 21562282]

Duncan JS, Fritzsch B. Transforming the vestibular system one molecule at a time: the molecular and developmental basis of vertebrate auditory evolution. Adv Exp Med Biol. 2012; 739:173–186. [PubMed: 22399402]

Duncan JS, Lim KC, Engel JD, Fritzsch B. Limited inner ear morphogenesis and neurosensory development are possible in the absence of GATA3. Int J Dev Biol. 2011; 55:297–303. [PubMed: 21553382]

Fay, R., editor. Hearing In Vertebrates: A Psychophysics Databook. Winnetka, IL: Hill-Fay Associates; 1988.

Fritzsch B. Inner ear of the coelocanth fish Latimeria has tetrapod affinities. Nature. 1987; 327:153–154. [PubMed: 22567677]

Fritzsch B, Beisel KW, Hansen LA. The molecular basis of neurosensory cell formation in ear development: a blueprint for hair cell and sensory neuron regeneration? Bioessays. 2006; 28:1181–1193. [PubMed: 17120192]

Fritzsch B, Eberl DF, Beisel KW. The role of bHLH genes in ear development and evolution: revisiting a 10-year-old hypothesis. Cell Mol Life Sci. 2010; 67:3089–3099. [PubMed: 20495996]

Fritzsch B, Jahan I, Pan N, Kersigo J, Duncan J, Kopecky B. Dissecting the molecular basis of organ of Corti development: Where are we now? Hear Res. 2011

Gifford RH, Revit LJ. Speech perception for adult cochlear implant recipients in a realistic background noise: effectiveness of preprocessing strategies and external options for improving speech recognition in noise. J Am Acad Audiol. 2010; 21:441–451. quiz 487-448. [PubMed: 20807480]

Groves AK, Fekete DM. Shaping sound in space: the regulation of inner ear patterning. Development. 2012; 139:245–257. [PubMed: 22186725]

Hertzano R, Puligilla C, Chan SL, Timothy C, Depireux DA, Ahmed Z, Wolf J, Eisenman DJ, Friedman TB, Riazuddin S, Kelley MW, Strome SE. CD44 is a marker for the outer pillar cells in the early postnatal mouse inner ear. J Assoc Res Otolaryngol. 2010; 11:407–418. [PubMed: 20386946]

Izumikawa M, Batts SA, Miyazawa T, Swiderski DL, Raphael Y. Response of the flat cochlear epithelium to forced expression of Atoh1. Hear Res. 2008; 240:52–56. [PubMed: 18430530]

Jacques BE, Montcouquiol ME, Layman EM, Lewandoski M, Kelley MW. Fgf8 induces pillar cell fate and regulates cellular patterning in the mammalian cochlea. Development. 2007; 134:3021–3029. [PubMed: 17634195]

Jahan I, Pan N, Kersigo J, Calisto LE, Morris KA, Kopecky B, Duncan JS, Beisel KW, Fritzsch B. Expression of Neurog1 instead of Atoh1 can partially rescue organ of Corti cell survival. PLoS One. 2012; 7:e30853. [PubMed: 22292060]

Jahan I, Pan N, Kersigo J, Fritzsch B. Neurod1 suppresses hair cell differentiation in ear ganglia and regulates hair cell subtype development in the cochlea. PLoS One. 2010; 5:e11661. [PubMed: 20661473]

Jones JM, Montcouquiol M, Dabdoub A, Woods C, Kelley MW. Inhibitors of differentiation and DNA binding (Ids) regulate Math1 and hair cell formation during the development of the organ of Corti. J Neurosci. 2006; 26:550–558. [PubMed: 16407553]

Jorgensen J, Locket N. The inner ear of the echidna Tachyglossus aculeatus: the vestibular sensory organs. Proc R Soc Lond B Biol Sci. 1995; 260:183–189.

Karis A, Pata I, van Doorninck JH, Grosveld F, de Zeeuw CI, de Caprona D, Fritzsch B. Transcription factor GATA-3 alters pathway selection of olivocochlear neurons and affects morphogenesis of the ear. J Comp Neurol. 2001; 429:615–630. [PubMed: 11135239]

Kiernan AE, Pelling AL, Leung KK, Tang AS, Bell DM, Tease C, Lovell-Badge R, Steel KP, Cheah KS. Sox2 is required for sensory organ development in the mammalian inner ear. Nature. 2005; 434:1031–1035. [PubMed: 15846349]

Kirjavainen A, Sulg M, Heyd F, Alitalo K, Yla-Herttuala S, Moroy T, Petrova TV, Pirvola U. Prox1 interacts with Atoh1 and Gfi1, and regulates cellular differentiation in the inner ear sensory epithelia. Dev Biol. 2008; 322:33–45. [PubMed: 18652815]

Kopecky B, Decook R, Fritzsch B. Mutational ataxia resulting from abnormal vestibular acquisition and processing is partially compensated for. Behav Neurosci. 2012a; 126:301–313. [PubMed: 22309445]

Kopecky B, Johnson S, Schmitz H, Santi P, Fritzsch B. Scanning thin-sheet laser imaging microscopy elucidates details on mouse ear development. Dev Dyn. 2012b; 241

Kopecky B, Santi P, Johnson S, Schmitz H, Fritzsch B. Conditional deletion of N-Myc disrupts neurosensory and non-sensory development of the ear. Dev Dyn. 2011; 240:1373–1390. [PubMed: 21448975]

Kopecky BJ, Decook R, Fritzsch B. N-Myc and L-Myc are essential for hair cell formation but not maintenance. Brain Research. 2012c; 1484:1–14. [PubMed: 23022312]

Kopecky BJ, Duncan JS, Elliott KL, Fritzsch B. Three-dimensional reconstructions from optical sections of thick mouse inner ears using confocal microscopy. J Microsc. 2012d; 248:292–298. [PubMed: 23140378]

Ladher RK, Wright TJ, Moon AM, Mansour SL, Schoenwolf GC. FGF8 initiates inner ear induction in chick and mouse. Genes Dev. 2005; 19:603–613. [PubMed: 15741321]

Laine H, Doetzlhofer A, Mantela J, Ylikoski J, Laiho M, Roussel MF, Segil N, Pirvola U. p19(Ink4d) and p21(Cip1) collaborate to maintain the postmitotic state of auditory hair cells, their codeletion leading to DNA damage and p53-mediated apoptosis. J Neurosci. 2007; 27:1434–1444. [PubMed: 17287518]

Lanford PJ, Shailam R, Norton CR, Gridley T, Kelley MW. Expression of Math1 and HES5 in the cochleae of wildtype and Jag2 mutant mice. J Assoc Res Otolaryngol. 2000; 1:161–171. [PubMed: 11545143]

Liu Z, Walters BJ, Owen T, Brimble MA, Steigelman KA, Zhang L, Mellado Lagarde MM, Valentine MB, Yu Y, Cox BC, Zuo J. Regulation of p27Kip1 by Sox2 Maintains Quiescence of Inner Pillar Cells in the Murine Auditory Sensory Epithelium. J Neurosci. 2012; 32:10530–10540. [PubMed: 22855803]

Mak AC, Szeto IY, Fritzsch B, Cheah KS. Differential and overlapping expression pattern of SOX2 and SOX9 in inner ear development. Gene Expr Patterns. 2009; 9:444–453. [PubMed: 19427409]

Mantela J, Jiang Z, Ylikoski J, Fritzsch B, Zacksenhaus E, Pirvola U. The retinoblastoma gene pathway regulates the postmitotic state of hair cells of the mouse inner ear. Development. 2005; 132:2377–2388. [PubMed: 15843406]

Masuda M, Dulon D, Pak K, Mullen LM, Li Y, Erkman L, Ryan AF. Regulation of POU4F3 gene expression in hair cells by 5' DNA in mice. Neuroscience. 2011; 197:48–64. [PubMed: 21958861]

Masuda M, Pak K, Chavez E, Ryan AF. TFE2 and GATA3 enhance induction of POU4F3 and myosin VIIa positive cells in nonsensory cochlear epithelium by ATOH1. Developmental Biology. 2012; 372:68–80. [PubMed: 22985730]

Matei V, Pauley S, Kaing S, Rowitch D, Beisel KW, Morris K, Feng F, Jones K, Lee J, Fritzsch B. Smaller inner ear sensory epithelia in Neurog 1 null mice are related to earlier hair cell cycle exit. Dev Dyn. 2005; 234:633–650. [PubMed: 16145671]

Montcouquiol M, Corwin JT. Brief treatments with forskolin enhance s-phase entry in balance epithelia from the ears of rats. J Neurosci. 2001; 21:974–982. [PubMed: 11157083]

Morsli H, Choo D, Ryan A, Johnson R, Wu DK. Development of the mouse inner ear and origin of its sensory organs. J Neurosci. 1998; 18:3327–3335. [PubMed: 9547240]

Muller M, von Hunerbein K, Hoidis S, Smolders JW. A physiological place-frequency map of the cochlea in the CBA/J mouse. Hear Res. 2005; 202:63–73. [PubMed: 15811700]

Nichols DH, Pauley S, Jahan I, Beisel KW, Millen KJ, Fritzsch B. Lmx1a is required for segregation of sensory epithelia and normal ear histogenesis and morphogenesis. Cell Tissue Res. 2008; 334:339–358. [PubMed: 18985389]

Oesterle EC, Chien WM, Campbell S, Nellimarla P, Fero ML. p27(Kip1) is required to maintain proliferative quiescence in the adult cochlea and pituitary. Cell Cycle. 2011; 10:1237–1248. [PubMed: 21403466]

Ohyama T, Groves AK. Generation of Pax2-Cre mice by modification of a Pax2 bacterial artificial chromosome. Genesis. 2004; 38:195–199. [PubMed: 15083520]

Pan N, Jahan I, Kersigo J, Duncan JS, Kopecky B, Fritzsch B. A novel Atoh1 "self-terminating" mouse model reveals the necessity of proper Atoh1 level and duration for hair cell differentiation and viability. PLoS One. 2012; 7:e30358. [PubMed: 22279587]

Pan N, Jahan I, Kersigo J, Kopecky B, Santi P, Johnson S, Schmitz H, Fritzsch B. Conditional deletion of Atoh1 using Pax2-Cre results in viable mice without differentiated cochlear hair cells that have lost most of the organ of Corti. Hear Res. 2011; 275:66–80. [PubMed: 21146598]

Pauley S, Kopecky B, Beisel K, Soukup G, Fritzsch B. Stem cells and molecular strategies to restore hearing. Panminerva Med. 2008; 50:41–53. [PubMed: 18427387]

Pauley S, Lai E, Fritzsch B. Foxg1 is required for morphogenesis and histogenesis of the mammalian inner ear. Dev Dyn. 2006; 235:2470–2482. [PubMed: 16691564]

Pauley S, Wright TJ, Pirvola U, Ornitz D, Beisel K, Fritzsch B. Expression and function of FGF10 in mammalian inner ear development. Dev Dyn. 2003; 227:203–215. [PubMed: 12761848]

Peterson NR, Pisoni DB, Miyamoto RT. Cochlear implants and spoken language processing abilities: review and assessment of the literature. Restor Neurol Neurosci. 2010; 28:237–250. [PubMed: 20404411]

Pirvola U, Spencer-Dene B, Xing-Qun L, Kettunen P, Thesleff I, Fritzsch B, Dickson C, Ylikoski J. FGF/FGFR-2(IIIb) signaling is essential for inner ear morphogenesis. J Neurosci. 2000; 20:6125–6134. [PubMed: 10934262]

Puligilla C, Kelley MW. Building the world's best hearing aid; regulation of cell fate in the cochlea. Curr Opin Genet Dev. 2009; 19:368–373. [PubMed: 19604683]

Raft S, Koundakjian EJ, Quinones H, Jayasena CS, Goodrich LV, Johnson JE, Segil N, Groves AK. Cross-regulation of Ngn1 and Math1 coordinates the production of neurons and sensory hair cells during inner ear development. Development. 2007; 134:4405–4415. [PubMed: 18039969]

Renton JP, Xu N, Clark JJ, Hansen MR. Interaction of neurotrophin signaling with Bcl-2 localized to the mitochondria and endoplasmic reticulum on spiral ganglion neuron survival and neurite growth. J Neurosci Res. 2010; 88:2239–2251. [PubMed: 20209634]

Riccomagno MM, Takada S, Epstein DJ. Wnt-dependent regulation of inner ear morphogenesis is balanced by the opposing and supporting roles of Shh. Genes Dev. 2005; 19:1612–1623. [PubMed: 15961523]

Rocha-Sanchez SM, Scheetz LR, Contreras M, Weston MD, Korte M, McGee J, Walsh EJ. Mature mice lacking Rbl2/p130 gene have supernumerary inner ear hair cells and supporting cells. J Neurosci. 2011; 31:8883–8893. [PubMed: 21677172]

Roehm PC, Hansen MR. Strategies to preserve or regenerate spiral ganglion neurons. Curr Opin Otolaryngol Head Neck Surg. 2005; 13:294–300. [PubMed: 16160524]

Ruben RJ. The synthesis of DNA and RNA in the developing inner ear. Laryngoscope. 1969; 79:546–556. [PubMed: 5821137]

Sage C, Huang M, Vollrath MA, Brown MC, Hinds PW, Corey DP, Vetter DE, Chen ZY. Essential role of retinoblastoma protein in mammalian hair cell development and hearing. Proc Natl Acad Sci U S A. 2006; 103:7345–7350. [PubMed: 16648263]

Tran BH. Endolymphatic deafness: a particular variety of cochlear disorder. ORL J Otorhinolaryngol Relat Spec. 2002; 64:120–124. [PubMed: 12021503]

Weber T, Corbett MK, Chow LM, Valentine MB, Baker SJ, Zuo J. Rapid cell-cycle reentry and cell death after acute inactivation of the retinoblastoma gene product in postnatal cochlear hair cells. Proc Natl Acad Sci U S A. 2008; 105:781–785. [PubMed: 18178626]

Webster, D.; Fay, R.; Popper, A., editors. The Evolutionary Bilogy of Hearing. Springer; 1992.

White PM, Doetzlhofer A, Lee YS, Groves AK, Segil N. Mammalian cochlear supporting cells can divide and trans-differentiate into hair cells. Nature. 2006; 441:984–987. [PubMed: 16791196]

Witte MC, Montcouquiol M, Corwin JT. Regeneration in avian hair cell epithelia: identification of intracellular signals required for S-phase entry. Eur J Neurosci. 2001; 14:829–838. [PubMed: 11576187]

Xiang M, Maklad A, Pirvola U, Fritzsch B. Brn3c null mutant mice show long-term, incomplete retention of some afferent inner ear innervation. BMC Neurosci. 2003; 4:2. [PubMed: 12585968]

Young SL, Diolaiti D, Conacci-Sorrell M, Ruiz-Trillo I, Eisenman RN, King N. Premetazoan ancestry of the Myc-Max network. Mol Biol Evol. 2011; 28:2961–2971. [PubMed: 21571926]

Zheng JL, Helbig C, Gao WQ. Induction of cell proliferation by fibroblast and insulin-like growth factors in pure rat inner ear epithelial cell cultures. J Neurosci. 1997; 17:216–226. [PubMed: 8987750]

- *N-Myc* can compensate for the loss of *L-Myc* during inner ear development but cannot be compensated for by *L-Myc*.
- The combined loss of *N-Myc* and *L-Myc* during early inner ear development results in a more dramatic phenotype than previously described with the loss of *N-Myc* alone.
- In the absence of both *N-Myc* and *L-Myc*, the timing between proliferation and differentiation in the inner ear is disrupted as shown by decreased mRNA levels of *Neurod1, Atoh1, Pou4f3*, and *Barhl1*, leading to cochlear hair cell death.

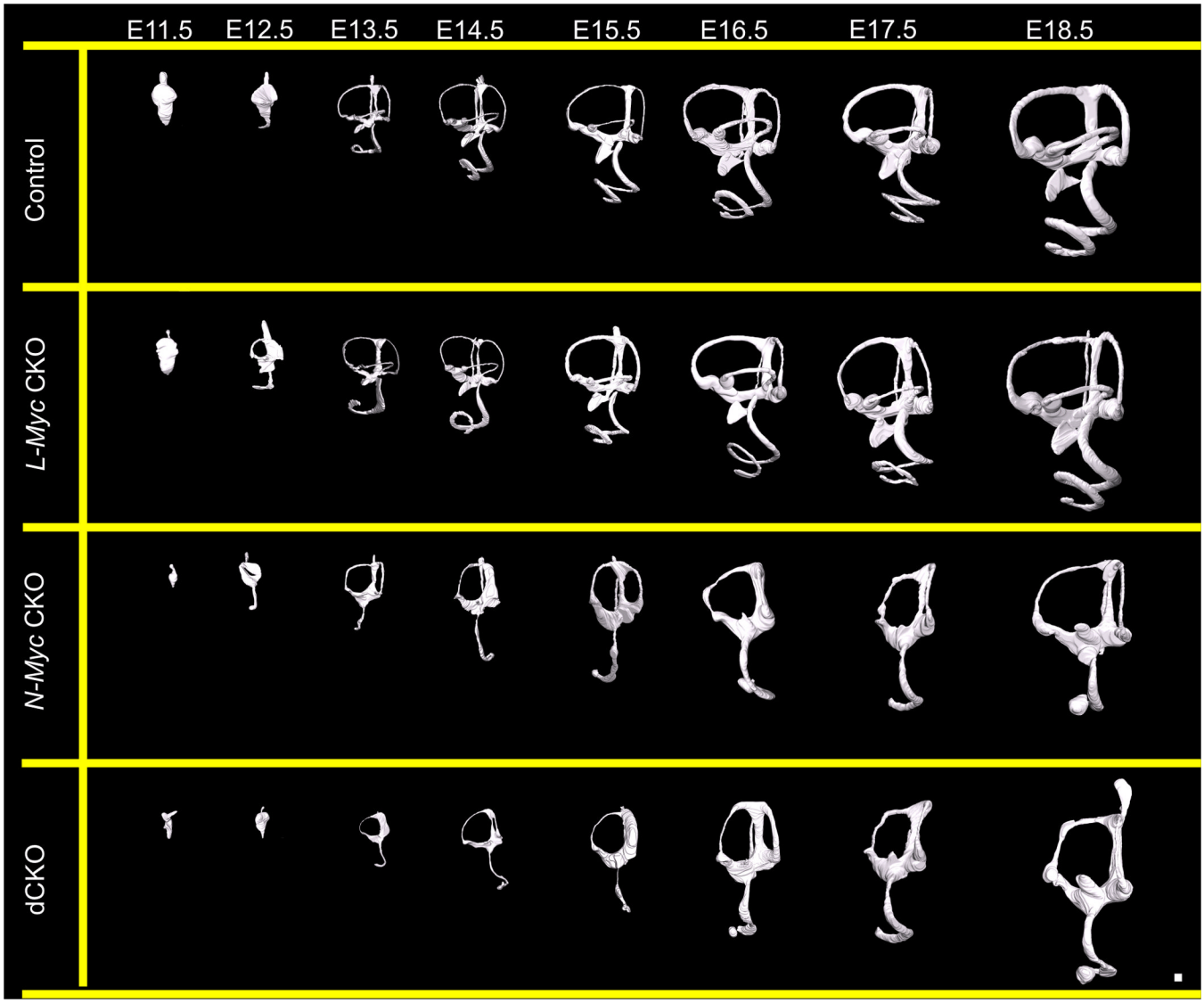

Figure 1. Three dimensional reconstructions to assess the development of the mouse inner ear in the absence of *N-Myc* and *L-Myc*

Using confocal microscopy followed by manual segmentation, three dimensional reconstructions are made of over 100 ears from E11.5 to E18.5 of control (row 1), *L-Myc* CKO (row 2), *N-Myc* CKO (row 3), and dCKO (row 4) ears. Shown are lateral views of the developing ear from an early polarity-defined otocyst to a three dimensional labyrinth with six distinct sensory recesses. By E16.5, the utriculosaccular foramen and ductus reuniens formed such that all recesses are distinguishable. The development of *L-Myc* CKO ears were similar to control with no distinct differences (compare row 1 and row 2). In the absence of *N-Myc, N-Myc* CKO ears show gross morphological abnormality starting early at E11.5 (row 3). The dCKO mice are overall very similar but have several additional defects relative to *N-Myc* CKO mice (row 4). In both mutant mice, the cochlea never fully extends and the apical tip forms at times, a disconnected sac-like structure (row 3 and 4). The saccular recess never forms and the saccular macula never separates from the cochlea through the formation of the hair cell free ductus reuniens (row 3 and 4). The horizontal canal and utriculosaccular foramen also do not develop (row 3 and 4). However, the dCKO

mice ears are even further reduced in size than *N-Myc* CKO mice and have a more severe vestibular phenotype with additional loss of posterior canal. Scale bar = 100μm.

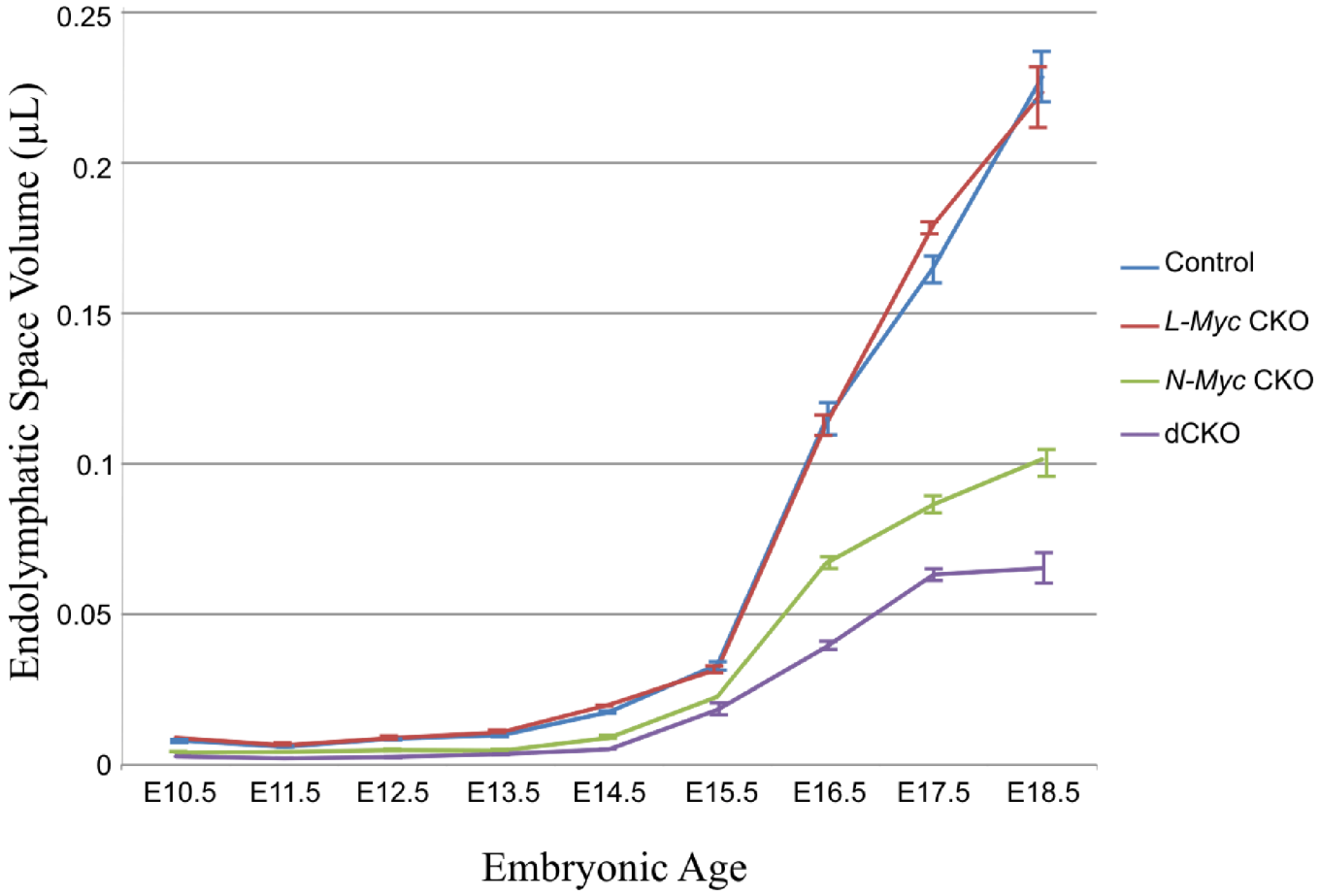

Figure 2. Comparisons of inner ear endolymphatic space development in absence of *N-Myc* and *L-Myc* by three dimensional reconstructions

In general, there is a slow increase in overall endolymphatic space from E10.5 to E15.5. However, from E15.5 to E18.5, after the formation of the utriculosaccular foramen and ductus reuniens, there is a dramatic increase in endolymphatic space in all ears. In all ages, *L-Myc* CKO (red) mice have very similar volumes as in control (blue). *N-Myc* CKO (green) and dCKO (purple) both mice have substantially reduced volumes at all time points, however this change is even more remarkable after E15.5 and the volume remains reduced more in dCKO compared to *N-Myc* CKO. Moreover, the endolymphatic space in dCKO mice was significantly reduced ($p<0.05$) compared to control at all time points except at E10.5 (as E10.5 dCKO N=1). Error bars are standard error of the mean. Number of ears at E10.5, E11.5, E12.5, E13.5, E14.5, E15.5, E16.5, E17.5, and E18.5 for control: 3,3,8,6,3,4,4,5,and 4; for *Pax2-Cre N-Myc f/+ L-Myc f/f*: 1,2,3,3,3,3,2,3, and 2; *Pax2-Cre N-Myc f/f L-Myc f/+*: 3,3,2,4,2,1,3,2, and 4; dCKO: 1,3,4,7,2,2,3,5, and 2.

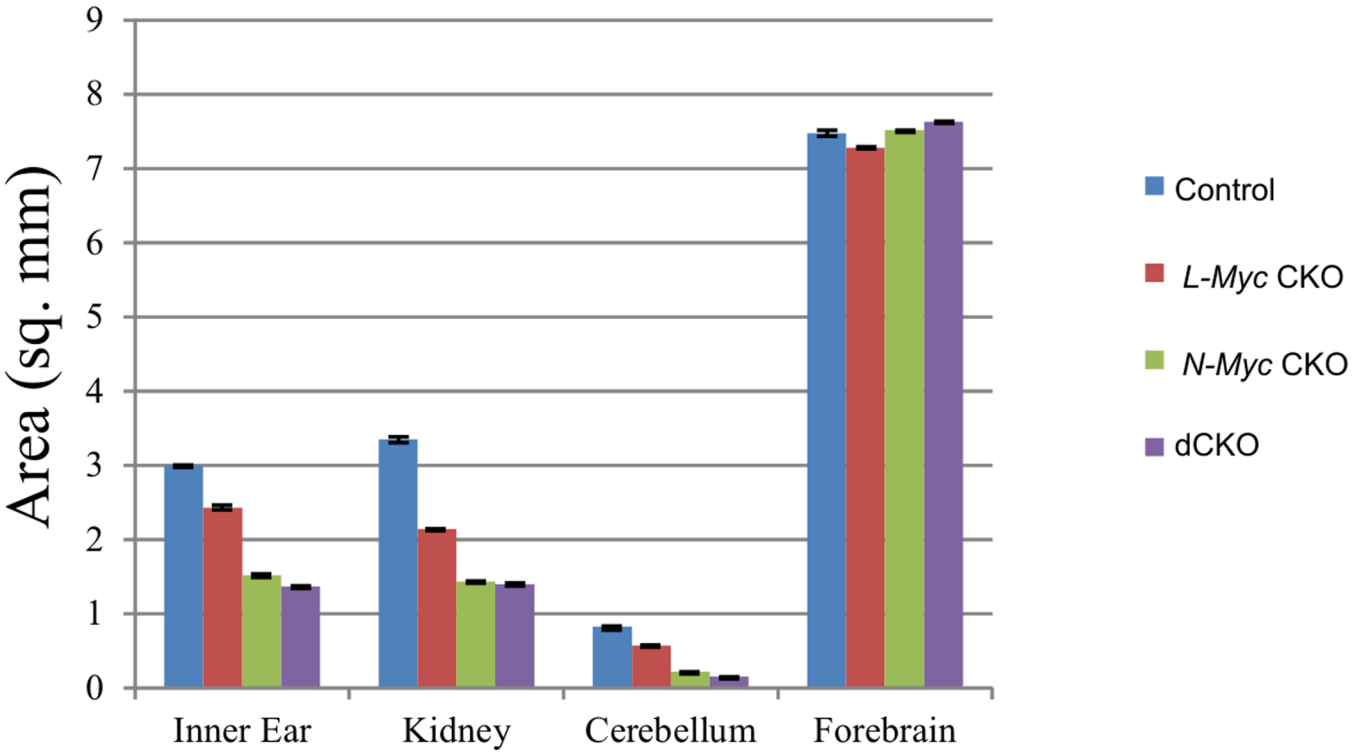

Figure 3. *N-Myc* has more effect than *L-Myc* in *Pax2*-expressing organ development

Pax2 is expressed in the inner ear, kidney and cerebellum but not in the forebrain. Area measurement of these organs in P0 control (blue), *L-Myc* CKO (red), *N-Myc* CKO (green) and dCKO (purple) mice reveal that all three mutant mice have decreased cross sectional area compared to control for *Pax2*-expressing regions, but there is no change in size of the forebrain, a non-*Cre* expressing region. In addition, *N-Myc* CKO and dCKO mice have greater size reduction than *L-Myc* CKO alone in all the *Pax2*-expressing regions. Error bars are standard error of the mean. N= 6 for each measurement.

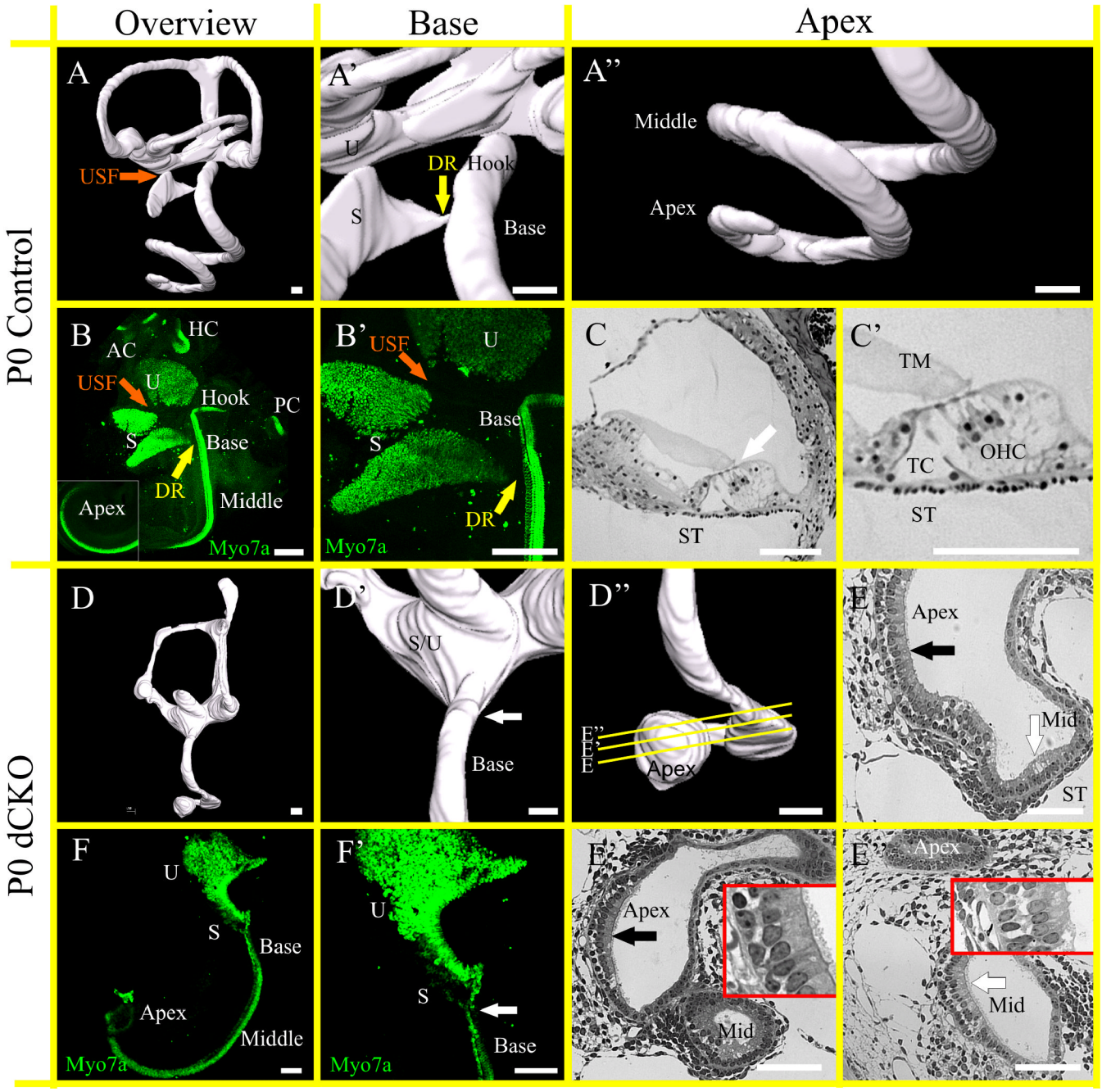

Figure 4. dCKO mice have a severely aberrant cochlea that is most profoundly affected at the base and apex

Three dimensional reconstructions of control (A–A") and dCKO (D–D") ears show that separation of the utricle and saccule with the utriculosaccular foramen (USF, orange arrow) and the saccule and base of the cochlea with the ductus reuniens (DR, yellow arrow) fail to form in the dCKO (D, D') compared to control (A, A'). The apical tip highlights the dramatically abnormal "ball" formation in the dCKO (compare A, A" with D, D''). In control, all six sensory epithelia are segregated, shown with Myo7a immunohistochemistry (B, B'), importantly the utricle, saccule, and base of the cochlea are separated with the formation of the USF (orange arrow) and DR (yellow arrow). Epoxy resin sections through

the apex in control (C, C') shows the tectorial membrane (TM) resting on top of the three rows of outer hair cells (OHC) and the single inner hair cell. The tunnel of Corti (TC) separates the Pillar cells. The white arrow indicates region of organ of Corti in C. In contrast to control, the dCKO mice have a fusion of the utricle and saccule that precludes any distinction between the two (F, F'). There is a reduction in size of the combined epithelia relative to the control (compare A with D). In control the base extends with the hook region (labeled 'Hook') past the point where the DR joins the cochlear duct (A', B). However, in dCKO there is no hook region of the cochlea and the base blends into the saccule, indicating that the entire high frequency end of late cell cycle exiting hair cells of the organ of Corti never forms (white arrows in D', F'). In addition, there is a coordinated reduction of four rows to hair cells to the single row of inner hair cells in control that is severely disrupted in dCKO and the base of the cochlea is fused with the saccule (F, F'). Serial sections of the ball-like apex show both vestibular-like hair cells (black arrow in E and E') sitting over the periotic mesenchyme. In contrast, the organ of Corti in control and in middle turn in dCKO is on top of periotic space, the scala tympani (ST). White arrow indicates presumed region of organ of Corti in E and E". 'Apex' indicates the ball-like region whereas 'Mid' is the forming middle turn. The ball-like apex is discontinuous with the middle turn (E'). The middle turn organ of Corti (white arrow in E'') is also abnormal. Magnified region in E' and E'' highlight areas indicated by black and white arrows, respectively. AC, anterior canal crista; HC, horizontal canal crista; PC, posterior canal crista; S, saccule and U, utricle. Scale bar = 100 μm.

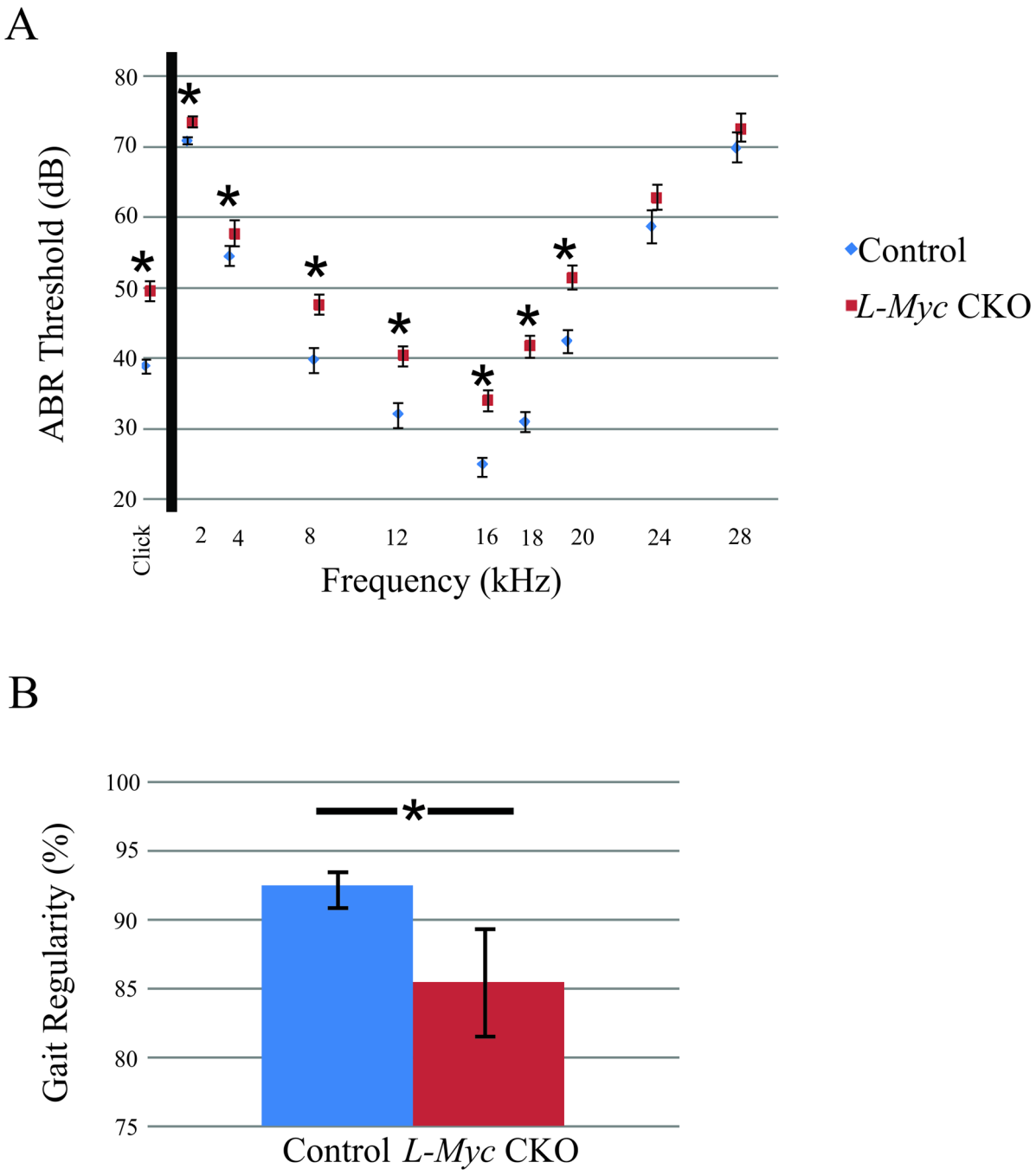

Figure 5. Loss of *L-Myc* results in some auditory and vestibulo-motor abnormalities

Auditory and vestibulo-motor functions are assessed using the ABR threshold and by the Catwalk system for the regularity of gait performance in the *L-Myc* CKO (N = 21 in ABR; N=11 in Catwalk) and control (N = 18 in ABR; N=33 in Catwalk) mice at P21. Despite *L-Myc* CKO mice has overall near normal development similar to control as shown in Figure 1–3, both the auditory and vestibulo-motor function are detected abnormal at P21 compared to control (A, B). The ABR demonstrates a significantly worse hearing than the control in the *L-Myc* CKO mice (A, $p<0.05$). The *L-Myc* CKO mice also suffers from gait abnormality as shown with the significant decrease in the gait regularity compared to control (B, $p<0.015$). Note that the three survived P21 N-Myc CKO mice are assessed for the ABR

and Catwalk, but no detectable ABR response are found at any frequency or sound level tested and are unable to walk in the Catwalk set-up and therefore data not included in the Figure 5. Error bars are standard error of the mean.

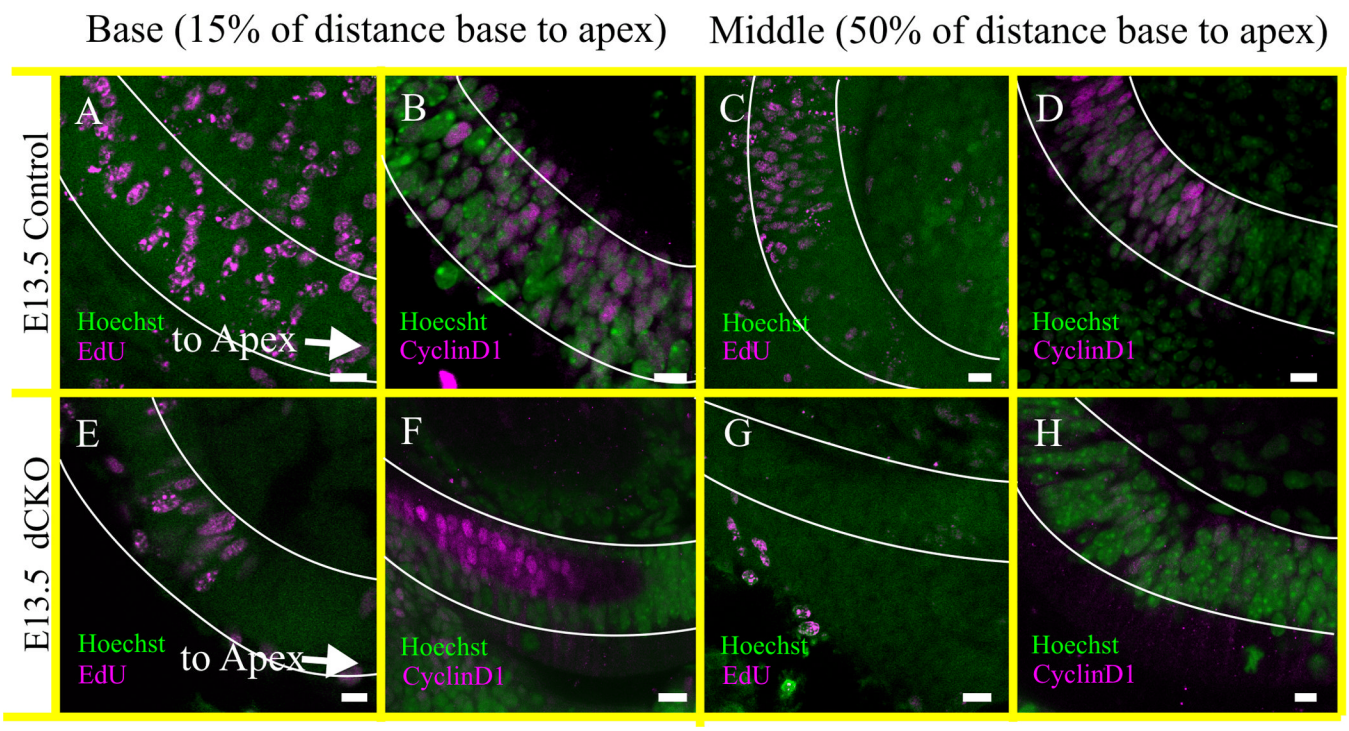

Figure 6. Proliferation ends prematurely in the cochlea of dCKO mice

The proliferation of the organ of Corti is assessed at E13.5 by the injection of EdU eight hours before collection at E13.5 (A,E,C,G). EdU positive staining is indicative of DNA synthesis and the proliferating cells are in the S phase of the cell cycle. The proliferation detected with the EdU is confirmed by the CyclinD1 immunohistochemistry at E13.5 mice (B,F,D,H) and both are co-labeled with the Hoechst nuclear stain (A–H). The proliferating cells are reduced in the 'basal part' of cochlea in the dCKO compared to control littermate shown by both EdU and CyclinD1 staining (compare A,B with E,F). However, in the 'middle' part of the cochlea, no EdU or CyclinD1 positive cells are detected in the dCKO mice (compare C,D with G,H). EdU and CyclinD1 positive cells are reduced in the 'middle' part of the control cochlea than that of the 'base' indicating a natural decline of proliferation by E13.5 which usually starts from apex at E12 (A–D) (Matei et al., 2005). In contrast, complete absence of EdU and CyclinD1 positive cells at 'middle' and reduction at 'base' already by E13.5 suggests the premature cessation of proliferation in the dCKO cochlea (E–H). The distribution of these cells are scored as 'base' if it was at 15% of the distance from the basal tip of the organ of Corti (outlined in white; A,B,E,F), and as 'middle' if it was near 50% of the distance between base and apex (outlined in white; C,D,G,H). Proliferation is not assessed in the vestibular organs. Scale bar = 10 μm.

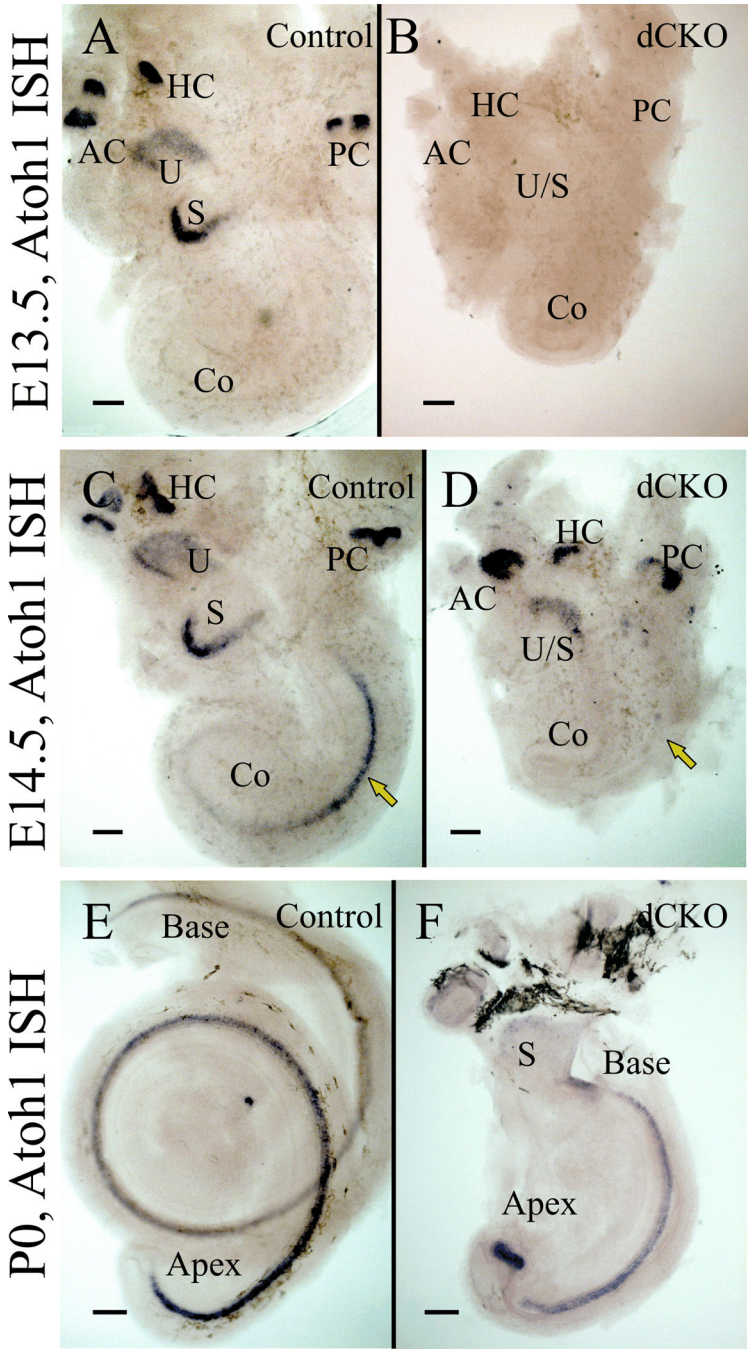

Figure 7. *In situ* hybridization of *Atoh1* shows delayed upregulation in dCKO mice

In situ hybridization of *Atoh1* in E13.5 control mice show that *Atoh1* mRNA is expressed in all vestibular epithelia but not yet in the cochlea (A). In matched littermates of E13.5 dCKO mice, *Atoh1* expression is not detected, not even in the vestibular epithelia (B). At E14.5, Atoh1 is upregulated in the mid-base of the cochlea in control mice (C). However, in the E14.5 dCKO, *Atoh1* is expressed only in the vestibular epithelia, but not in the cochlea (D). Atoh1 expression is thus delayed in the dCKO mice for at least one day in the vestibular epithelia and likely in the cochlea as well (compare A,B with C,D). By P0, *Atoh1* is expressed in the entire cochlea in both control (E) and dCKO littermates (F). However, in the dCKO, there is a gap in expression between the middle turn and apex with an aberrant

and profound upregulation of *Atoh1* in the ball-like apical tip. AC, anterior canal crista; Co, cochlea; HC, horizontal canal crista; PC, posterior canal crista; S, saccule and U, utricle. Scale bar = 100 μm.

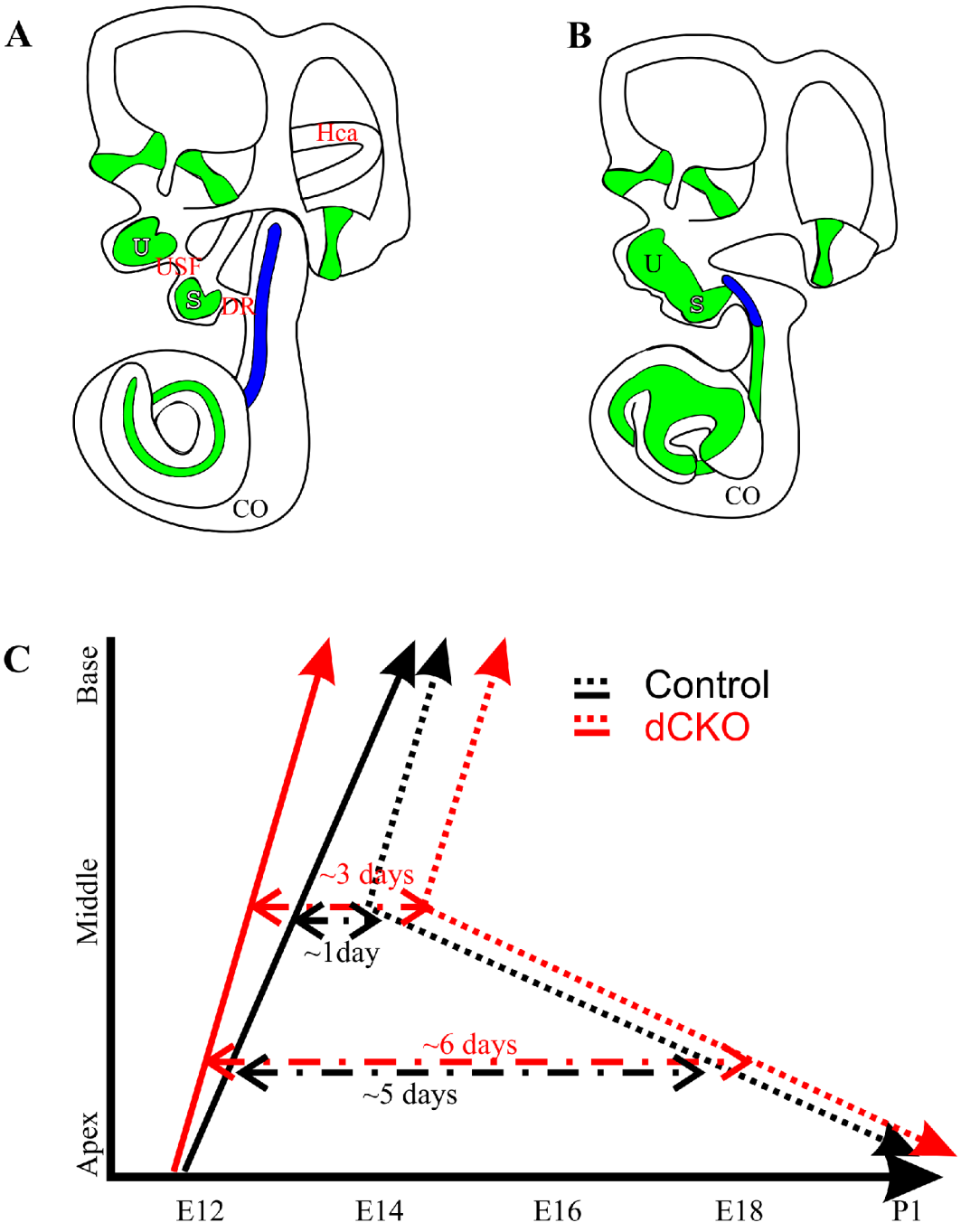

Figure 8. Loss of *Myc*'s affects cell cycle exit, onset of *Atoh1* expression and inner ear differentiation

This diagram shows the morphological alterations in the inner ear of control and dCKO mutant mice at E13.5 (A,B) and alterations in proliferation and onset of *Atoh1* expression based on the data generated here and in previous publications (C). Note the loss of the horizontal canal (HC), utriculosaccular foramen (USF), ductus reuniens (DR), the fusion of utricle and saccule (U,S), the shortened cochlea (CO) with the malformed apex and the restriction of cell cycle exit to shorter basal part (Blue) in the dCKO mice (B) compared to control mice (A). Previous data showed that hair cells exit the cell cycle in the apex around E12, at the middle turn at E13 and at the base at E14.5 in control mice (black line, C). We

previously showed that proliferation is restricted to the apical half cochlea after E12.5 injection of EdU (Kopecky et al., 2011) and have similar data on dCKO's. At E13.5 cochlear proliferation is in the base and middle turn (Fig. 6). In contrast, in the dCKO, limited proliferation is restricted to the base with no proliferation in the middle turn by E13.5 (Fig. 6). This indicates that the cell cycle exit in the dCKO is accelerated at least one day. It is nearly ceased in the E13.5 cochlea (Fig. 6, red line in C). We presented here this cell cycle exit points as a straight lines with black representing control and red the dCKO, indicating cell cycle exit progressing from apex to base. The dotted lines represent the expression onset of *Atoh1* as revealed here and in other publications with black representing control and red dCKO (Matei et al., 2005; Pan et al., 2012). Note that *Atoh1* expression starts in the mid-base of the cochlea around E13–14 (dependent on nomenclature used and mouse strains involved) and progresses toward both the base and the apex (black dotted line in C). While the basal tip shows *Atoh1* expression about a day after it can be detected in the mid-base, the apical tip has a delayed onset of expression until early neonates (black dotted line in C). *Atoh1* expression shows a delayed onset of at least one day in the dCKO compared to control (Fig. 7, red dotted line in C). Combined these data suggest that lack of *Myc*'s has two effects: it accelerates the cell cycle exit and delays the onset of *Atoh1*. This exposes the hair cells along the cochlea with a variable time delay between cell cycle exit with an increase of around 1–2 days before *Atoh1* expression starts (dashed lines). Data are compiled after (Ruben, 1969; Lanford et al., 2000; Chen et al., 2002; Matei et al., 2005; Kopecky et al., 2011; Pan et al., 2012) and present data.

Table 1

Changes of gene expression in the dCKO are shown by qRT-PCR analysis (Mean+/−SEM). The dCKO values are normalized to control value of “1”.

Gene	E11.5	E12.5	E13.5	E14.5	E15.5	P0
N-Myc	0.21+/−0.074*	0.14+/−0.040*	0.14+/−0.033*	0.19+/−0.042*	0.16+/−0.080*	0.12+/−0.027*
L-Myc	0.16+/−0.061*	0.28+/−0.061*	0.24+/−0.046*	0.22+/−0.076*	0.15+/−0.094*	0.13+/−0.023*
ID2	0.46+/−0.074*	0.56+/−0.17	0.47+/−0.060*	0.44+/−0.064*	0.47+/−0.091*	0.63+/−0.037
ID3	1.21+/−0.26	1.25+/−0.41	0.66+/−0.024*	0.87+/−0.13	1.37+/−0.31	0.46+/−0.033
Neurod1	0.56+/−0.076	0.56+/−0.088*	0.66+/−0.10	0.41+/−0.043*	0.42+/−0.11*	0.32+/−0.033*
Atoh1	0.36+/−0.12*	0.43+/−0.070*	0.26+/−0.060*	0.71+/−0.096*	0.80+/−0.14	0.79+/−0.043*
Pou4f3	0.34+/−0.033*	0.37+/−0.049*	0.35+/−0.19	0.54+/−0.051*	0.51+/−0.12*	0.37+/−0.10*
Barhl1	0.22+/−0.099*	0.25+/−0.12*	0.73+/−0.21	0.78+/−0.092	0.61+/−0.26	0.51+/−0.079*
E2F2	0.71+/−0.080	1.87+/−0.99	1.83+/−0.30	0.66+/−0.082*	0.50+/−0.099*	
E2F4	0.55+/−0.072*	0.87+/−0.13	0.25+/−0.015*	0.56+/−0.056*	0.49+/−0.049*	0.50+/−0.029
RB	0.86+/−0.074	0.35+/−0.035*	0.90+/−0.034	0.70+/−0.062*	0.87+/−0.18	0.55+/−0.0065*
P27Kip1	0.45+/−0.026*	0.68+/−0.081*	0.12+/−0.047*	0.31+/−0.070*	0.278+/−0.035*	0.08+/−0.023*
CyclinD2	0.86+/−0.13	0.84+/−0.15	1.27+/−0.41	0.79+/−0.16	1.31+/−0.32	0.81+/−0.011
Pax2	0.61+/−0.22	0.38+/−0.022*	0.50+/−0.13*	0.27+/−0.047*	0.46+/−0.13*	0.27+/−0.012*
Fgf8	0.85+/−0.22	0.68+/−0.054*	0.52+/−0.089*	0.44+/−0.069*	0.28+/−0.074*	0.36+/−0.11
Sox2	0.59+/−0.076*	0.61+/−0.077*	1.00+/−0.15	0.42+/−0.069*	0.57+/−0.061*	
Gata3	0.63+/−0.27	0.62+/−0.13*	0.76+/−0.20	0.34+/−0.030*	0.57+/−0.13*	0.44+/−0.025*
N	4	6	4	6	5	4

The genes that are significantly reduced in the dCKO compared to control are indicated with the ‘*’.

* indicates $p < 0.05$.

Numbers of mice used in each time points are indicated by ‘N’.